JOURNAL OF FOOD PROCESS ENGINEERING

D.R. HELDMAN
and
R.P. SINGH
COEDITORS

FOOD & NUTRITION PRESS, INC.

VOLUME 16, NUMBER 4

DECEMBER 1993

JOURNAL OF FOOD PROCESS ENGINEERING

All articles for publication and inquiries regarding publication should be sent to DR. D.R. HELDMAN, COEDITOR, *Journal of Food Process Engineering,* Food Science/Engineering Unit, University of Missouri-Columbia, 235 Agricultural/Engineering Bldg., Columbia, MO 65211 USA; or DR. R.P. SINGH, COEDITOR, *Journal of Food Process Engineering,* University of California, Davis, Department of Agricultural Engineering, Davis, CA 95616 USA.

All subscriptions and inquiries regarding subscriptions should be sent to Food & Nutrition Press, Inc., 2 Corporate Drive, P.O. Box 374, Trumbull, CT 06611 USA.

One volume of four issues will be published annually. The price for Volume 16 is $127.00 which includes postage to U.S., Canada, and Mexico. Subscriptions to other countries are $147.00 per year via surface mail, and $156.00 per year via airmail.

Subscriptions for individuals for their own personal use are $97.00 for Volume 16 which includes postage to U.S., Canada, and Mexico Personal subscriptions to other countries are $117.00 per year via surface mail, and $126.00 per year via airmail. Subscriptions for individuals should be sent direct to the publisher and marked for personal use.

The *Journal of Food Process Engineering* (ISSN: 0145-8876) is published quarterly (March, June, September and December) by Food & Nutrition Press, Inc.—Office of Publication is 2 Corporate Drive, P.O. Box 374, Trumbull, Connecticut 06611 USA.

Second class postage paid at Bridgeport, CT 06602.

POSTMASTER: Send address changes to Food & Nutrition Press, Inc., 2 Corporate Drive, P.O. Box 374, Trumbull, CT 06611.

JOURNAL OF FOOD PROCESS ENGINEERING

Journal of FOOD PROCESS ENGINEERING

VOLUME 16
NUMBER 4

Coeditors: D.R. HELDMAN
R.P. SINGH

FOOD & NUTRITION PRESS, INC.
TRUMBULL, CONNECTICUT 06611 USA

ISSN 0145-8876

Printed in the United States of America

CONTENTS

RELATION OF BACTERIAL DESTRUCTION TO CHEMICAL MARKER FORMATION DURING PROCESSING BY THERMAL PULSES[1]

EDWARD W. ROSS

Department of Mathematical Sciences
Worcester Polytechnic Institute
100 Institute Road
Worcester, MA 01609-2280

Accepted for Publication April 21, 1993

ABSTRACT

This paper presents a formulation in dimensionless terms of the equations pertaining to first-order processes that follow Arrhenius kinetics, and applies them to problems in food thermoprocessing. The need for it arose from attempts to understand the relation between destruction of pathogenic microorganisms and formation of chemical markers in the food. During processing food is subjected to a thermal pulse that affects the markers and microorganisms. The dimensionless formulation makes it convenient to obtain equations expressing the relation between the decadic reduction in microbial population and the rise in marker concentration for temperature-time profiles of forms hitherto not conveniently calculable. Measurements of chemical markers can be used with these formulas to predict destruction of microorganisms. Examples are given of calculations demonstrating the feasibility of this approach when a single marker is monitored.

INTRODUCTION

The effect of variable temperature on chemical and biological changes, and consequently on food processing, has been studied for a long time. The effect of temperature on the rates of change of constituents or microorganisms is usually well represented by the Arrhenius relationship, whose form, however, makes it difficult to estimate the amount of change that occurs when the temperature is not constant but varies with time. In a very common situation the

[1]Correspondence Address: Edward W. Ross, 152 Barton Drive, Sudbury, MA 01776.

food is subjected to a temperature history in the form of a pulse, consisting of heating and cooling phases separated by a holding period of constant temperature. Most ordinary processes require estimation of the contributions from the heating and cooling phases. The extent of thermal processing has been estimated approximately for several forms of temperature variation, notably constant, linear, sinusoidal and exponential behaviors. These solutions are usually accurate enough when the temperature range is not too great but risk imprecision in other circumstances.

The general theory governing time-temperature effects in food processing is described in books by Ball and Olson (1957), Labuza (1982), Lund (1975), Singh and Heldman (1984) and Stumbo (1973). Among the many papers dealing with variable temperatures are Diendoerfer and Humphrey (1959), Hayakawa (1970, 1978), Labuza (1979, 1984), Labuza and Kamman (1983), Nunes *et al.* (1991), Rhim *et al.* (1989), Senum and Yang (1977) and Swartzel (1982). Teixeira *et al.* (1969a, b, 1975) have examined the effect of spatial as well as temporal variations of temperature on thiamine retention during processing.

The present paper begins by deriving an apparently new set of exact formulas for food processing when the temperature undergoes pulse-like variation with time. The time histories for which this is done are approximately those of a power law. The impetus for the study came from attempts to comprehend the relation between chemical marker formation and microorganism destruction during food processing. The development is entirely mathematical, although the purpose is to clarify certain questions in food processing.

In recent years, as the means of chemical detection have improved, considerable interest has arisen concerning chemical markers, i.e., substances that are formed naturally in the food at known rates during processing. With chemical markers the hope is that measurements of such compounds can convey useful information about the temperature time history of the food in a container during processing. One such marker has been identified and its parameters measured by Kim and Taub (1993). Chemical markers perform a function similar to time-temperature indicators, which have been studied by Wells and Singh (1988) and Hendrickx *et al.* (1992), and are possibly of value in applications to continuous retort systems and to heat exchangers, holding tubes and suspended particulate behavior in ultra high temperature (UHT) processing, see Sapru *et al.* (1992) and David and Merson (1990).

At the present time there is a need to demonstrate the kind of information that can be obtained from chemical marker measurements and to define the properties that such a marker ought to have. The exact solutions given here contribute to answering these questions with some clarity and generality. For example, if the properties of a putative marker are known, it is possible to decide whether measuring its yield will give adequate and reliable information about microbial destruction or inactivation.

This study begins with a consistent reformulation in dimensionless guise of the familiar equations describing food processing under variable temperatures. The crucial step in this development is the definition of a dimensionless, inverse temperature in terms of an initially defined reference temperature. Exact values of the processing are found for thermal pulses whose dimensionless, inverse temperatures have power-law profiles in time. These values allow us to find the desired relation between microbial population and marker concentrations and to discern the effects of processing parameters on this relationship. Numerical examples are given of these calculations.

THEORETICAL BACKGROUND

The mathematical parameters to be used in this exposition are defined as follows. N(t), the population of the microorganism of interest (e.g., *Clostridium botulinum* or *Bacillus stearothermophilus*), depends on time, t, as a first order process, i.e., it obeys the differential equation

$$dN/dt = -k_n[T(t)]N \tag{1}$$

The rate constant, k_n, depends on absolute temperature, T, which in turn depends on time.

The solution of this equation at final time t_f is

$$N(t_f) = N_o\, e^{-\sigma(t_f)} \tag{2}$$

where $$\sigma(t_f) = \int_0^{t_f} k_n[T(t)]dt = \ln[N_o/N(t_f)] \tag{3}$$

assuming that $N = N_o$ at the initial time, t = 0. The effect of temperature on the rate constant is taken as given by the Arrhenius relationship,

$$k_n[T(t)] = k_{on}e^{[-E_{an}/\{RT(t)\}]}$$

where R is the universal gas constant and E_{an} and k_{on} are, respectively, the activation energy and preexponential factor for the microorganism.

We now express these relations in dimensionless form by first introducing an absolute reference temperature, T_r, and then defining the following:

$$E_n = E_{an}/(RT_r) \tag{4}$$
$$x = (T_r/T) - 1 \quad \text{or} \quad T = T_r/(1 + x) \tag{5}$$

E_n is now dimensionless activation energy, and x is a dimensionless inverse transformation of T, i.e., x decreases as T increases. Then

$$E_{an}/(RT) = [E_{an}/(RT_r)][T_r/T] = E_n(1 + x)$$

and the Arrhenius relationship and (4) and (5) lead to

$$k_n = k_{rn}e^{(-E_n x)} \qquad (6)$$

where $$k_{rn} = k_{on}e^{(-E_n)}$$

Equation (5) implies that when $T = T_r$, $x = 0$, so that k_{rn} is the rate constant at the reference temperature, T_r, because of Eq. (6). In dimensionless terms, Eq. (3) becomes

$$\sigma(t_f) = k_{rn}F(t_f) \qquad (7)$$

where $$F(t_f) = \int_0^{t_f} e^{[-E_n x(t)]}dt \qquad (8)$$

$F(t_f)$ has the dimension of time. When T is constant, x is constant and

$$F(t_f) = t_f e^{(-E_n x)}$$

This formula is used to calculate F during the holding phase of a thermal process. If $T = T_r$, then $x = 0$ and $F(t_f) = t_f$.

Since the time dependence of N is determined by σ, and therefore by F, all temperature histories that give the same value of $F(t_f)$ will lead to the same value of $N(t_f)$. $F(t_f)$ is a measure of the microorganism destruction that takes place during time t_f. Much of this paper is devoted to the estimation of $F(t_f)$ (which under certain circumstances is also called F_o) for various profiles of the surrogate temperature, x(t).

The reference temperature may be chosen as any convenient value for the situation under study. In food processing, T_r would usually be taken as 394.1K or 121.1C. For most foods E_n is a rather large number, typically exceeding 20. Also, since the range of temperatures in processing is frequently much less than T_r it is often true that $|x| \ll 1$, and so the binomial approximations are

$$T \approx T_r(1 - x) \text{ and } x \approx 1 - (T/T_r) \qquad (9)$$

reasonable. Approximations of this sort are widely made in the food science literature; they are not used here but are helpful in visualizing the inverse relationship between T and x.

If T is constant, then x is constant, and Eq. (8) gives

$$\sigma(t_f) = \ln[N_o/N(t_f)] = k_{rn}t_f e^{(-E_n x)}$$

The quantity D_T, the time (at temperature T) for which $N_o/N(t_f) = 10$, is often referenced in food processing work. From the above,

$$k_{rn}D_T e^{(-E_n x)} = B = \ln(10) = 2.303$$

In particular, when $T = T_r$, $x = 0$ and

$$D = D_r = B/k_{rn} \tag{10}$$

This leads to the relation

$$\begin{aligned} F(t_f) = (\sigma/k_{rn}) &= D_r[(1/B)\ln(N_o/N)] \\ &= D_r\log_{10}(N_o/N) \end{aligned}$$

which is a formula sometimes used to calculate F_o.

Another quantity often used in describing food processes is z, defined so that $-z$ is the temperature decrease (K) required to reduce k_{rn} to $k_{rn}/10$. Since Eq. (6) implies

$$k_n = (k_{rn}/B)10^{(-E_n x)}$$

it is easily seen that x_z, the x-value that reduces k_{rn} to $k_{rn}/10$, is given by

$$x_z = B/E_n \tag{11}$$

Transforming this back to temperatures, we obtain

$$T_z = T_r E_n/(E_n+B) = T_r - z$$

which is solved to find

$$z = T_r B/(E_n+B) \quad \text{or} \quad E_n = B[(T_r/z) - 1] \tag{12}$$

If $E_n \gg B$, then approximately

$$z \approx T_rB/E_n = BRT_r^2/E_{an}$$

in agreement with the usual formula.

The relationship between F and the usual formula for F_0 can be seen by starting with the integrand of F in Eq. (8) and using the definition of B to obtain

$$e^{-E_n x} = 10^{-E_n x/B}$$

The exponent of 10 in this formula is, because of Eq. (4),

$$-E_{an}x/(RT_rB)$$

The above approximate formula for z can be rewritten as

$$E_{an}/(RT_rB) = T_r/z$$

and used to find the exponent of 10,

$$-T_rx/z \approx -T_r[1 - (T/T_r)]/z \approx [T - T_r]/z$$

with the aid of Eq. (9). If T_r is taken as 394.1K or 121.1C, this is identical with the customary exponent of 10 in the integrand for F_0. The F defined by Eq. (8) is slightly more general than F_0, so a slightly different symbol is used for it.

To this point, we have obtained formulas pertaining to N. The markers obey analogous formulas. The concentration, M, of the marker, formed from an indigenous precursor, is assumed to obey the first-order differential equation

$$dM/dt = k_m[T(t)]\,(M_\infty - M)$$

which has the solution

$$M(t_f) = M_\infty\{1 - e^{[-\alpha(t_f)]}\}$$

where $$\alpha(t_f) = \int_0^{t_f} k_m[T(t)]\,dt = -\ln[1-M(t_f)/M_\infty] \quad (13)$$

M_∞ is the limiting marker-concentration achieved after extensive processing, and k_m is the rate constant for formation of the marker. The dependence of rate constant on temperature for the marker is assumed to obey the Arrhenius relationship with activation energy E_{am} and preexponential constant k_{om}. The transformation to dimensionless variables for M is analogous to that for N. k_{rm} is the rate constant when $T = T_r$, and E_m is dimensionless activation energy,

$$E_m = E_{am}/(RT_r) \tag{14}$$

By analogy with the formulas for N, we obtain

$$k_m = k_{rm}e^{(-E_m x)}, \quad k_{rm} = k_{om}e^{(-E_m)}$$

$$\alpha(t_f) = k_{rm}F_m(t_f) \tag{15}$$

$$F_m(t_f) = \int_0^{t_f} e^{[-E_m x(t)]}dt \tag{16}$$

If more than one marker is present, the foregoing definitions apply to each. The markers are distinguished by replacing the subscript m by a numerical subscript. Thus, for two markers, E_m is designated, respectively, E_1 and E_2, k_{rm} becomes k_{r1} and k_{r2}, and so on.

CALCULATION OF σ AND α FOR THERMAL PULSES

In this section we develop formulas by which the integral, $F(t_f)$, can be estimated for thermal pulses of many different profiles. These are characterized by formulas expressed in terms of x(t). Because the contribution to $F(t_f)$ of the holding phase is easily found from

$$F(t_f) = t_f e^{(-E_n x)}$$

it will be ignored, and the pulse taken as consisting only of a rise followed by a fall in temperature. Moreover, as Hayakawa (1970) has shown, processing during cooling is the same as that during heating when the profile is symmetric. It is therefore necessary only to calculate the F-value for the cooling phase, for which x increases; the same F-value will result during a symmetric heating phase, and twice that F-value is the total for the entire symmetric pulse.

POWER-LAW PULSES

The temperature-time profile during the cooling phase of the pulse is assumed to be

$$x(t) = x_p + h(t - t_p)^a$$

and
$$h = (x_o - x_p)/(t_f - t_p)^a$$

where the phase begins at $t = t_p$ with $x = x_p$ and ends at $t = t_f$ where $x = x_o$. It is assumed that $a > 0$, $t_f > t_p$ and $x_p < x_o$, so that x increases (and T decreases). If E is the dimensionless activation energy of either marker or microorganism, we evaluate

$$I = \int_{t_p}^{t_f} e[-Ex(t)]dt$$

$$I = e[-Ex_p] \int_{t_p}^{t_f} e[-Eh(t - t_p)^a] \; dt$$

Defining $L = (Eh)^{1/a}$, and $u = \{L(t - t_p)\}^a$

leads, after some manipulation, to

$$I = (La)^{-1} e^{(-Ex_p)} \int_0^{\{L(t_f-t_p)\}^a} e^{-u} u^{[(1/a)-1]} du$$

The integral is known to be the Incomplete Gamm Function, γ, [see Abramowitz and Stegun (1964)], and so

$$I = (La)^{-1} e^{(-Ex_p)} \gamma[1/a, \{L(t_f - t_p)\}^a]$$

This expression can be written in more succinct form by defining

$$w = \{L(t_f - t_p)\}^a = E(x_o - x_p), \quad \beta = 1/a \tag{17}$$

and observing that $1/L = (t_f - t_p) w^{-\beta}$:

$$I/[t_f-t_p] = e^{(-Ex_p)} \beta w^{-\beta} \gamma(\beta, w) \tag{18}$$

Abramowitz and Stegun (1964) describe the properties of $\gamma(\beta,w)$.

It is also convenient to define

$$F_p = (t_f - t_p)\ e^{(-Ex_p)}$$

so that F_p is the processing that would result from a rectangular pulse, i.e., the constant, peak temperature, x_p, applied during the time of processing. Then the ratio of the processing for a power-law pulse to that of a rectangular pulse is

$$r = I/F_p = \beta\ w^{-\beta}\ \gamma(\beta,\ w) \tag{19}$$

The function r is exhibited graphically in Fig. 1.

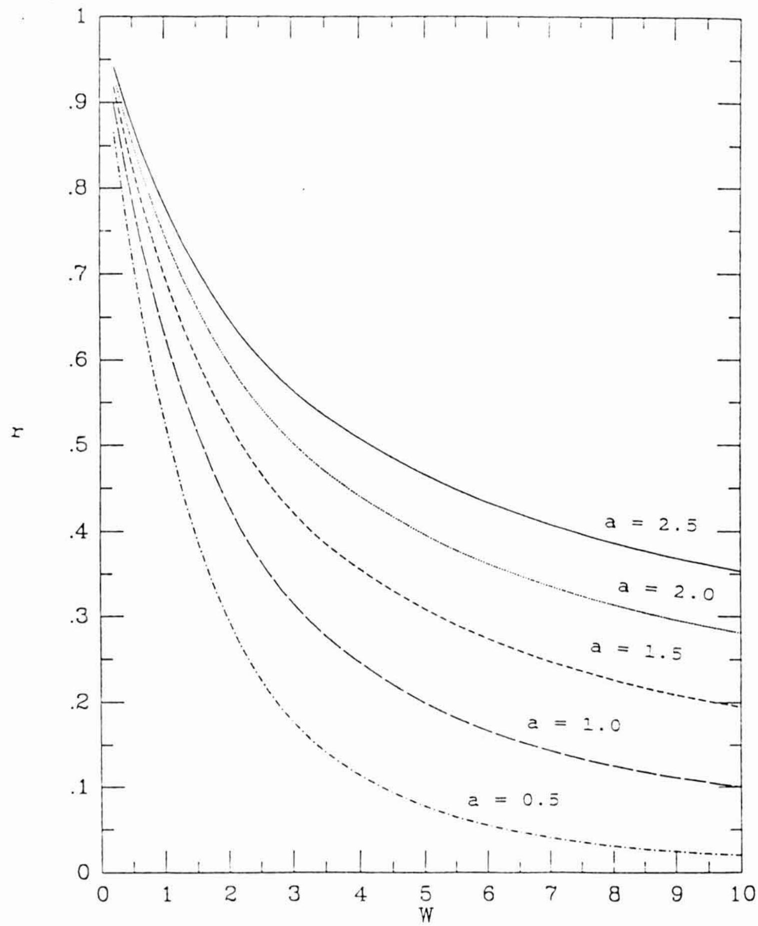

FIG. 1. r AS A FUNCTION OF w FOR VARIOUS VALUES OF SHAPE FACTOR $a = 1/\beta$: _._._, a = 0.5; __ __ __. a = 1.0; ---, a=1.5; ...., a = 2.0; _______, a = 2.5

It is helpful to record simpler, approximate formulas for r, based on the behavior of $\gamma(\beta, w)$, that are valid when $|w| \ll 1$,

$$r \approx 1 - \beta w/(1+\beta) + \beta w^2/(4+2\beta)$$

and, when $|w| \gg 1$,

$$r \approx w^{-\beta}\Gamma(1+\beta) - (\beta/w)e^{-w} \tag{20}$$

$\Gamma(\beta)$ denotes the (complete) Gamma Function, $\Gamma(\beta) = \gamma(\beta,\infty)$. The latter (asymptotic) approximation is very useful. Moreover, its second term can be neglected, i.e.,

$$r \approx w^{-\beta}\Gamma(1+\beta) \tag{21}$$

with less than 5% error when $w > 1 + 2\beta$.

A very useful special case of these formulas is when a = 2 and $\beta = 1/2$, namely a pulse for which x is quadratic in t. Then Abramowitz and Stegun (1964) state that

$$\gamma(1/2,w) = \sqrt{\pi}\ \mathrm{erf}(w^{1/2})$$

which, through Eq. (19), implies

$$r \approx C\ w^{-1/2}\ \mathrm{erf}(w^{1/2}), \qquad C = \pi^{1/2}/2$$

A further simplification, as in Eq. (21) above, is often possible. If $w > 2$, less than 5% error is committed if we merely set $\mathrm{erf}(w^{1/2}) = 1$. This approximation is discussed in the Section on Numerical Examples and is seen to be almost always acceptable in processing situations for a = 2. The estimate for the quadratic pulse is then

$$r \approx Cw^{-1/2}$$

and Eq. (17) leads to

$$I \approx (C/g)(t_f - t_p)\ e^{(-Ex_p)}$$

where $$g = w^{1/2} = [E(x_o - x_p)]^{1/2}$$

To obtain $F(t_f)$ for a complete, symmetric, quadratic pulse, we have to multiply this by 2, and use $t_f = 2t_p$, so

$$F(t_f) = t_f(C/g)e^{(-Ex_p)} \tag{22}$$

The estimates of $\sigma(t_f)$ and $\alpha(t_f)$ are found by combining Eq. (7), (15) and (22) to obtain

$$\sigma(t_f) = k_{rn}t_f(C/g_n)e^{(-E_n x_p)} \tag{23}$$

where $$g_n = [E_n(x_o - x_p)]^{1/2}$$

and $$\alpha(t_f) = k_{rm}t_f(C/g_m)e^{(-E_m x_p)} \tag{24}$$

where $$g_m = [E_m(x_o - x_p)]^{1/2}$$

These will be used in the next Section to estimate σ from measurements of α for a symmetric, quadratic pulse.

ESTIMATING MICROBIAL DESTRUCTION FROM MARKER FORMATION

In this section we use the formulas derived above for quadratic pulses to see what information about destruction of microorganisms can be obtained from measurements on the formation of intrinsic chemical markers.

Equations (23) and (24) imply that at $t = t_f$, i.e., at the end of processing,

$$\sigma/\alpha = (k_{rn}/k_{rm})(g_m/g_n)\ e^{[(E_m - E_n)x_p]}$$

or $$\sigma = \alpha(k_{rn}/k_{rm})(E_m/E_n)^{1/2}\ e^{[(E_m - E_n)x_p]} \tag{25}$$

We see that if α is measured, the only remaining parameters in the formula for σ are the rate constants, k_{rn} and k_{rm}, the dimensionless activation energies, E_n and E_m, and the dimensionless peak temperature (minimum $x = [T_r/T] - 1$), x_p. The rate constants and activation energies for the marker and microorganism will always be known in any practical situation, and so only x_p, which corresponds to the peak temperature, is unknown.

Equation (25) implies that, if the microorganism and marker have identical properties, i.e., $k_{rm} = k_{rn}$ and $E_m = E_n$, then $\sigma = \alpha$, and measurements of α would give directly the value of σ, regardless of x_p. If $k_{rm} \neq k_{rn}$, but $E_m = E_n$, the estimation of σ from measurements of α would again not require knowledge of x_p. If $E_m \neq E_n$, as is usually the case, the situation is more difficult.

If x_p is known, Eq. (25) allows one to calculate σ from measurements of α. Under many circumstances x_p may be known or assumed. If x_p is unknown, one must make measurements on two (or more) different markers to calculate σ. Both markers can be assumed to receive the same temperature pulse as the microorganism, and the formation of both markers can be expressed by the same formulas except for the parameter values, which we now distinguish by the subscripts 1 and 2. If M_1 and M_2 are, respectively, the concentrations of the two markers, $M_{1\infty}$ and $M_{2\infty}$ their limiting concentrations, E_1 and E_2 their dimensionless activation energies and k_{r1} and k_{r2} their rate constants at reference temperature T_r, Eq. (24) leads to

$$\begin{aligned} \alpha_1 &= -\ln[1 - (M_1/M_{1\infty})] \\ &= k_{r1}(C/g_1)t_f\, e^{(-E_1 x_p)} \qquad (26) \\ g_1 &= [E_1(x_o - x_p)]^{1/2} \end{aligned}$$

and

$$\begin{aligned} \alpha_2 &= -\ln[1 - (M_2/M_{2\infty})] \\ &= k_{r2}(C/g_2)t_f e^{(-E_2 x_p)} \qquad (27) \\ g_2 &= [E_2(x_o - x_p)]^{1/2} \end{aligned}$$

Then

$$\alpha_1/\alpha_2 = (k_{r1}/k_{r2})(E_2/E_1{}^{1/2})e^{[(E_2-E_1)x_p]}$$

This can be solved for x_p,

$$x_p = \ln\{\alpha_1/\alpha_2)(k_{r2}/k_{r1})(E_1/E_2)^{1/2}\}/(E_2-E_1) \qquad (28)$$

and σ can then be found from Eq. (25). In order to find x_p from measurements of α_1 and α_2, it is necessary only that $E_1 \neq E_2$, i.e., the two markers must not have the same activation energies. It would be wasteful, of course, to monitor two markers with equal parameters because, apart from statistical considerations, they would give no more information than one marker.

Equation (28) for x_p can be combined with Eq. (25)–(27) to furnish two formulas that give estimates for σ in terms of α_1 and α_2,

$$\sigma = (k_{rn}/\sqrt{E_n})\, H_1{}^{1-V}\, H_2{}^{V}$$

or

$$H = H_1(H_2/H_1)^V \qquad (29)$$

where

$$H = (\sigma/k_{rn})\sqrt{E_n}$$
$$H_1 = (\alpha_1/k_{r1})\sqrt{E_1}, \quad H_2 = (\alpha_2/k_{r2})\sqrt{E_2}$$
$$V = (E_n - E_1)/(E_2 - E_1)$$

Equations (29) describe completely the calculations that must be made when x_p is unknown or cannot be estimated. Some informal computer simulations suggest that these formulas give stable and useful predictions of σ in most practical cases, although the accuracy obviously depends on the parameter values (particularly $E_2 - E_1$) and also on the reliability of the quadratic assumption for x(t). This deserves further investigation.

RESULTS AND DISCUSSION

In this section we give a few examples of numerical calculations that illustrate the use of the foregoing formulas. These calculations use the parameter values, measured by Kim and Taub (1993), for marker, M-1, and microorganisms *Clostridium botulinum* (C. bot.) and *Bacillus stearothermophilus* (B. stear.) listed in Table 1. The reference temperature is taken as T_r = 394.1K (121.1C or 250F), and the gas constant as R = 1.987 cal/mol/K. The values given for D_r and z are taken from Lund (1975), and E_a and k_r are calculated from D_r and z by using Eq. (12), (4) and (10).

TABLE 1.
PARAMETERS FOR MARKER M-1; *BOTULINUM* AND *B. STEAROTHERMOPHILUS*

	Marker	B. stear.	C. bot.
D_{250} (min)	152.5	2.0	0.21
z (K)	27.9	12.0	9.88
E_a (kcal/mol)	23.7	57.4	69.3
k_r(1/min)	0.0151	1.1515	10.96
E (Dimensionless)	30.3	73.3	88.5

Symmetric Quadratic Pulse

The first example assumes a symmetric, quadratic pulse in x(t). Figure 2 shows the results as a plot of $\log_{10}(N_o/N)$ versus M/M_∞ for maximum temperatures between 250F (121.1C) and 270F (132.2C), based on Eq. (25). The parameters for M are those for the marker M-1 and for N those of microorganism *C. botulinum* (see Table 1). Then Eq. (25) leads to

$$\log_{10}(N_o/N) = 184.4\ e^{(-58.2x_p)}[-\ln\{1-(M/M_\infty)\}]$$

Figure 3 displays a similar plot for the same marker and *B. stearothermophilus*, governed by

$$\log_{10}(N_o/N) = 21.29\ e^{(-43.0x_p)}[-\ln\{1-(M/M_\infty)\}]$$

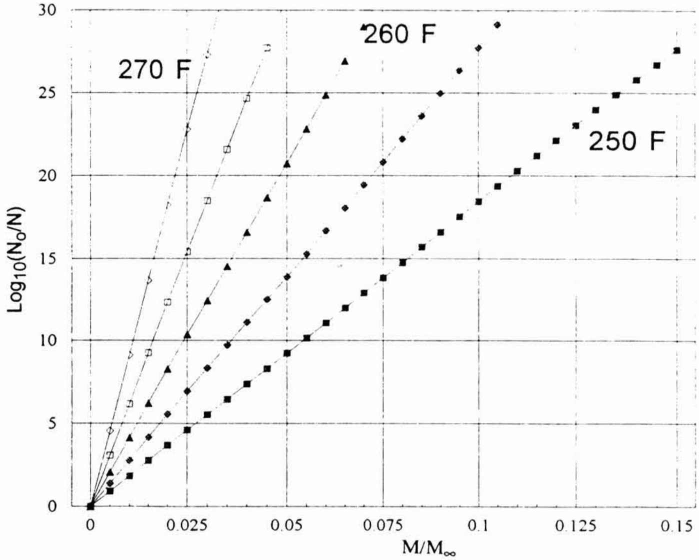

FIG. 2. PREDICTIVE GRAPH FOR DECADIC REDUCTION OF *C. BOTULINUM*
Fraction of marker formed, M/M_∞, for peak temperatures 250F, 255F, 260F, 265F and 270F

These graphs and formulas make explicit the prediction of N_o/N from measurements of the markers, provided the maximum temperature is known.

Plots like these are useful in assessing the practicality of making predictions using the marker. For example, this marker is reliably measureable only in the range $0.01 < M/M_\infty < 0.15$, with relative absolute error thought not to exceed 10%. The crucial range for C. bot. is usually $6 < \log_{10}(N_o/N) < 24$. It is important that these two ranges overlap, so that marker measurements are accurate when predicting relevant microbial destruction. Figures 2 and 3 show that the ranges overlap, so the marker can be expected to give accurate and useful predictions of process effectiveness as reflected in the decadic reduction of these microbial populations. Suppose, for example, that the marker measurements gave $M/M_\infty = 0.04$ and the maximum temperature was known to be 260F (126.7C); then for C. bot. Eq. (25) or Fig. 2 shows that $N_o/N \approx 10^{16.9}$. For B. stear. we conclude from Fig. 3 that $N_o/N \approx 10^{1.3}$, reflecting the smaller thermal sensitivity of B. stear.

Another way of representing the results for the quadratic pulse consists of displaying the behavior of the quantity

$$A = (\sigma/\alpha)(k_{rm}/k_r) = (E_m/E_n)^{1/2} e[(E_m - E_n)x_p]$$

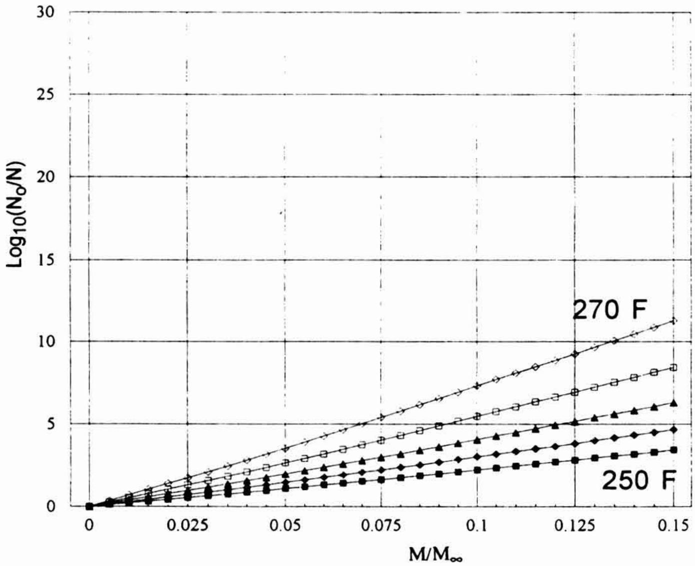

FIG. 3. PREDICTIVE GRAPH FOR DECADIC REDUCTION OF *B. STEAROTHERMOPHILUS*
$\text{Log}_{10}(N_o/N)$ vs. Fraction of Marker Formed, M/M_∞, for Peak Temperatures 250F, 255F, 260F, 265F and 270F.

for a particular marker, namely the one whose parameters are given in Table 1. A is the ratio of logarithmic bacterial destruction to logarithmic marker formation, scaled by the ratio of the rate constants at the reference temperature. The resulting graph, Fig. 4, shows how A depends on the maximum temperature and activation energy, $E = E_n$, of a microorganism co-existing with the M-1 marker when subjected to a quadratic pulse. For this very practical range of peak temperatures and E_n-values, A is seen to satisfy $0.2 \leq A \leq 3$, and therefore becomes neither pathologically large nor small. Again this suggests that these formulas lead to usable results.

Asymmetric Pulse

The second example illustrates the use of the power-law solution, Eq. (19), in estimating $F(t_f)$ for B. stear. when subjected to the temperature pulse shown in Fig. 5. This pulse corresponds to the following assumptions about x(t):

(1) The temperature starts at 355.2K (82.2C or 180F), rises to a maximum of 394.1K (121.1C or 250F) after $t_p = 10$ min, then returns to the initial temperature after a total of 14 min. Consequently, Eq. (5) leads to $x_p = 0$ and

$x_o = 0.1094$. During both heating and cooling, Eq. (17) implies that

$$w = E_n(x_o - x_p) = E_n x_o = 8.022$$

(2) During cooling [increasing x(t)] $a = 0.8$, $\beta = 1.25$ and $t_f - t_p = 4$.

(3) During heating [decreasing x(t)] the processing is the same as for a cooling phase having $a = 2.3$, $\beta = 0.4348$ and $t_f - t_p = 10$.

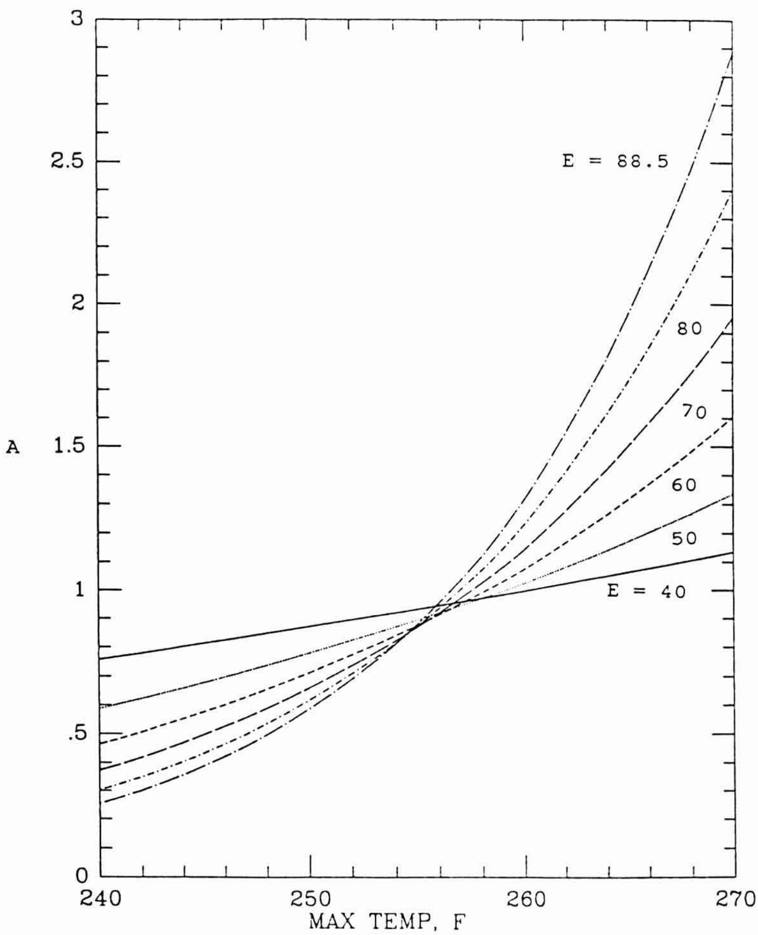

FIG. 4. A = (σ/α) (k_m/k_r) AS A FUNCTION OF MAXIMUM TEMPERATURE, (F) FOR FIXED MARKER, M-1, AND VARIOUS VALUES OF E = E_n, DIMENSIONLESS ORGANISM ACTIVATION ENERGY
__.__.__, E = 88.5; _._._. E = 80; __ __ __ E = 70; ----- E = 60; ..... E = 50; __ E = 40.

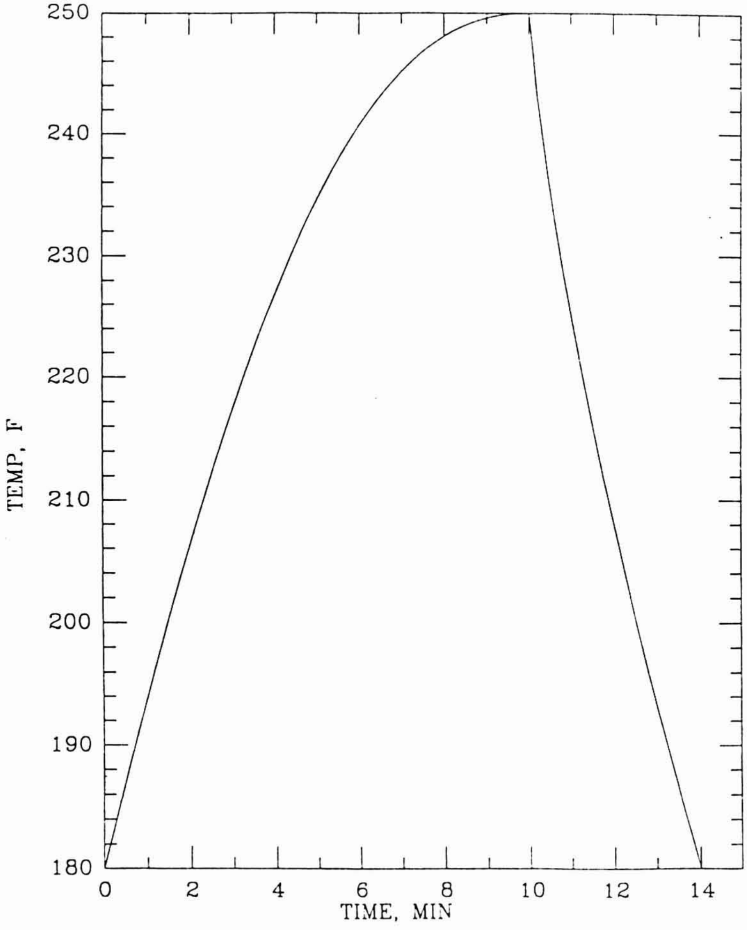

FIG. 5. UNSYMMETRIC TEMPERATURE-TIME PROFILE: TEMPERATURE (F) VS. TIME (MIN)

Because $w \gg 1 + 2\beta$, it is accurate to use Eq. (21) to find r during both heating and cooling. During heating

$$r = r_h \approx w^{-\beta}\Gamma(1+\beta) \approx 8.022^{-0.4348}[\Gamma(1.4348)] = 0.358$$

and similarly, during cooling

$$r = r_c \approx 8.022^{-1.25}[\Gamma(2.25)] = 0.0839.$$

Then, during heating and cooling, respectively, from Eq. (19)

$$I_h = F_p r_h = 10\ r_h = 3.58$$
$$I_c = 4r_c = 0.336.$$

Finally, the complete pulse is equivalent to

$$F(t_f) = I_h + I_c = 3.58 + 0.336 = 3.92 \text{ min}$$

at the reference temperature, 394.1K (121.1C). It is important to notice that the pulse in this example is not symmetric, but the same general formulas, Eq. (17) and (19), can be applied separately to the heating and cooling phases.

Accuracy of erf(g) ≈ 1

We might inquire whether the approximation erf(g) ≈ 1, made to obtain Eq. (22), is accurate during a typical food process. Taking 82.2C (355.2K) and 115.6C (388.6K) as initial and maximum temperatures, we find for a quadratic pulse with T_r = 394.1K,

$$x_o = 0.1094,\ x_p = 0.0143$$

For marker M-1, Eq. (17) implies w = 2.882, $g_m = \sqrt{w} = 1.698$, and a table of the Error Function shows that erf(g_m) increases as g_m increases and

$$\text{erf}(\sqrt{w}) = \text{erf}(g_m) = 0.984$$

Thus, the error committed in replacing erf(g_m) by 1 is less than 2%. For either of the two microorganisms (and the same temperature range) $E_n > E_m$, $g_n > g_m$, erf(g_n) > erf(g_m) and the error is smaller than for the marker. Also, if the temperature range is increased, so is x_o - x_p, and again g_m is made larger and erf(g_m) is nearer 1. It appears, therefore, that the approximation made in arriving at Eq. (22) is sufficiently accurate in the cases studied here.

GENERAL CONSIDERATIONS

The dimensionless formulation outlined in the Theoretical Background Section makes it possible to find various solutions for calculating bacterial destruction by the thermal pulses described above. The basic formula, Eq. (19), is exact even for very wide temperature ranges, unlike many solutions in the literature, which are accurate only when the temperature range is narrow enough. The solution is applicable at any point or small region in a food container for which the temperature history has the assumed form. In thermal processing the solution would be most relevant at the center or point of slowest heating. Spatial variation of bacterial destruction is only implicitly predicted.

A slight drawback to the solution of Eq. (19) is the somewhat recondite nature of the Incomplete Gamma Function. Tables of $\gamma(\beta,w)$ are not readily available, but it can be evaluated from a table of the Chi-Square Probability Distribution Function, P, which is related to $\gamma(\beta,w)$ by

$$\gamma(\beta,w) = \Gamma(\beta)\, P(2w\,|\,2\beta)$$

$P(2w\,|\,2\beta)$ is tabulated in Abramowitz and Stegun (1964) and many statistical books. A Fortran routine (GAMI) for calculating $\gamma(\beta,w)$ is available in the IMSL software and was used to generate Fig. 1. However, it appears that for many purposes the relatively simple approximations, Eq. (20) and especially (21), are adequate.

It is interesting that the asymptotic approximation to r for the power-law pulse, $r \approx w^{-\beta}\,\Gamma(1 + \beta)$, becomes more accurate as the range of temperatures becomes larger, i.e., $x_o - x_p$ increases. This behavior is diametrically opposite to that of the approximation, Eq. (9), which becomes more accurate as the range becomes smaller.

One advantage of having solutions by formula is that the effects of the various parameters are easily discerned. For example, in the case of the power-law pulse, r depends only on $w = E(x_o - x_p)$ when the shape parameter a (or β) is known. For the quadratic case, when these results are used to find σ/α, Eq. (25) shows that neither t_f nor x_o affects the relation between microbial destruction and marker formation. That x_O has no effect is a consequence of little or no processing occurring at the lower temperatures when the temperature range is large enough. Although this insensitivity to x_O is only true in an approximate sense (it results from setting erf(g) = 1), and is hardly surprising, it helps to have it made clearly visible.

Concerning the asymmetric pulse calculation of Example 2 above, some care is necessary if one attempts to check the computation by numerically integrating the customary formula for F_o. The results are likely to depart slightly from the values given above for at least four reasons: 1. The customary formula uses the approximation of Eq. (9), which is avoided in the present formulas. 2. The customary formula calculates z from E_n by the approximate formula

$$z = BT_r \,/\, E_n$$

instead of the formula used here,

$$z = BT_r/(E_n + B).$$

3. The approximation, Eq. (21), was used instead of the exact solution, Eq. (19). 4. The slope of the temperature-time profile is very steep at the start of cooling; numerical integration, which is sufficiently accurate elsewhere, may be unreliable in that region. Neither of the first two errors would be intolerable alone; indeed both approximations are widely and successfully used. The third relative error is extremely small, less than 4 x 10^{-5}. The last error is probably the most serious. If the errors were to add, the total error could be noticeable, though not probably more than 10%. However, it is unclear how the errors might combine.

The estimates of the relation between microbial destruction and marker formation derived above are based on the assumption of a symmetric, quadratic pulse in the dimensionless inverse temperature, x(t). A more general analysis, for any power law pulse, is possible, based on Eq. (21), but was deferred for the sake of simplicity. Though the quadratic behavior does not correspond exactly to any of the temperature profiles commonly studied (e.g., linear or exponential), it is a reasonable, but perhaps coarse, approximation to pulse-like temperatures at the center of a food container during retort or aseptic processing. The conclusions based on quadratic behavior are likely to hold for generally similar temperature profiles, although the numerical predictions will obviously vary. The more general power-law is capable of representing a considerable range of behaviors, and Fig. 5 suggests that some of these behaviors are quite realistic. Also, linear time-dependence is well approximated by the special case $a = \beta = 1$.

It is interesting that Fig. 4 shows an "equivalence point" phenomenon resembling that of Swartzel (1982). That is, the curves for different E-values nearly intersect at the same point, where the temperature is approximately 256F or 124.4C and A = 0.9. Swartzel's result appears to develop from the assumption of an exponential time-temperature curve, while the current result emerges from quadratic, inverse temperature behavior. The resemblance between them supports the notion that the occurrence of an equivalence point is not restricted solely to one form of temperature history.

The current interest in ultra high temperature processing, where the temperature range is large and exposure times are short, raises many interesting questions, both experimental and theoretical. The solution family found here, which is exact for the assumed temperature profile, whatever the temperature range, may be helpful in this context. Although it is occasionally awkward to deal with the Incomplete Gamma Function, it seems useful to have an entire family of exact solutions, upon which to base studies about the effects of changes in temperature profiles and chemical parameters.

The procedure used here for reducing the basic Equation (3) to dimensionless form appears to have certain advantages in simplifying the calculations that have to be done. It is inconvenient that the surrogate temperature, x, has an inverse rather than direct relation to absolute temperature, T, of which it is merely a mathematical transformation. However, if all the computations are done in terms of x, and the reversion to T introduced only after these are finished, the inverseness of their relation should not cause great difficulty. It should be understood, however, that the gain in convenience from this transformation is peculiar to the Arrhenius relation. If the kinetics do not follow the Arrhenius relation, this transformation may be valueless, although a different transformation to dimensionless form could perhaps be found that would yield similar benefits.

It appears that more study and experimentation are needed in order to determine the accuracy and sensitivity of this approach. To this purpose, experiments are now in progress at U.S. Army Natick RDT&E Center, using alginate beads inoculated with B. stear., placed in ham and chicken cubes and subjected to aseptic or near aseptic processing.

ACKNOWLEDGMENT

The author is pleased to acknowledge the financial support and technical cooperation of the U.S. Army Natick RD&E Center, Natick MA 01761 through the U.S. Army Research Office Scientific Services Program with Battelle-Research Triangle Park, NC, Work Order No. 2433. In particular, the insight and assistance of Dr. I. A. Taub played a major role in this effort. Also, discussions with Dr. K. Kustin, Chemistry Dept., Brandeis University, and Dr. Hie-Joon Kim of Natick were most valuable to the author. Finally, the author is indebted to the referees for their thoughtful and constructive comments.

NOMENCLATURE

A	Ratio of logarithmic bacterial destruction to logarithmic marker formation
a	Shape parameter (power) in temperature-time profile
B	$\log_e(10) \sim 2.303$
C	$\pi^{1/2}/2 \sim 0.8862$
D_r	Decimating time for organism at ref. temperature
D_T	Decimating time for organism at temperature T
E_n	Dimensionless activation energy for organism death
E_m, E_1, E_2	Dimensionless activation energies for marker formation
E_{an}	Activation energy for organism death
E_{am}	Activation energy for marker formation

erf	Error function
F	Equivalent processing time at ref. temperature
F_p	F for a rectangular pulse
g	Constant = $[E(x_o - x_p)]^{1/2}$
g_n, g_m	Constants g for organism and marker
g_1, g_2	Constants g for first and second markers
H	Function $(\sigma/k_{rn})\sqrt{E_n}$
H_1, H_2	Functions $(\alpha_1/k_{r1})\sqrt{E_1}$ and $(\alpha_2/k_{r2})\sqrt{E_2}$
h	Multiplicative constant in temperature-time profile
I	F integral over cooling phase of processing
I_h, I_c	F integral over heating and cooling phases
k_m	Rate constant for marker formation
k_n	Rate constant for death of microorganisms
k_{om}	Preexponential constants for marker
k_{on}	Preexponential constants for microorganism
k_{rn}	Rate constant for organism at reference temperature
k_{rm}, k_{r1}, k_{r2}	Rate constants for marker formation at reference temperature
L	Constant in integral calculation = $(Eh)^{1/a}$
M	Marker concentration
M_1, M_2	Concentrations of two markers
M_∞	Marker concentration limit as t tends to
$M_{1\infty}$, $M_{2\infty}$	Limit concentrations of two markers
N	Microorganism population or concentration
N_o	Initial microorganism population at time t_o
$P(2w \mid 2\beta)$	Chi-Square Probability Distribution Function
R	Universal Gas Constant, 1.987 cal/mol/K
r	Ratio of Integrals = I/F_p
r_h, r_c	Ratio r calculated for heating and cooling phases
T	Temperature
T_r	Reference (Ref.) Temperature, K
T_z	$T_r - z$
t	time
t_f	Final time
t_p	Time at peak temperature
u	Variable in transformation of integral I
V	Constant in Eq. 29, = $(E_n - E_1)/(E_2 \sim E_1)$
w	Constant = $E(x_o - x_p) = g^2$
x	Dimensionless, inverse temperature = $(T_r/T) - 1$
x_o, x_p	Initial x, and x at peak temperature
x_z	x-value that reduces k_{rn} to $k_{rn}/10$
z	Temperature decrease that reduces k_{rn} to $k_{rn}/10$

Greek Symbols

α, α_1, α_2	Rate integrals for marker formation
β	Constant in temperature-time profile, = 1/a
Γ	(Complete) Gamma Function
γ	Incomplete Gamma Function
σ	Rate integral for destruction of organism

REFERENCES

ABRAMOWITZ, M. and STEGUN, I.A. 1964. *Handbook of Mathematical Functions*, U.S. National Bureau of Standards, U.S. Printing Office, Washington, DC.

BALL, C.O. and OLSON, F.C.W. 1957. *Sterilization in Food Technology*, McGraw-Hill Book Co., New York.

DAVID, J.R.D. and MERSON, R.L. 1990. Kinetic parameters for inactivation of *Bacillus stearothermophilus* at high temperatures. J. Food Sci. *55*, 488.

DIENDOERFER, F.H. and HUMPHREY, A.E. 1959. Microbiological process discussion, analytical method for calculating heat-sterilization times. Appl. Microbiol. *7*, 256.

HAYAKAWA, K.I. 1970. Experimental formulas for accurate estimation of transient temperature of food and their application to thermal process evaluation. Food Technol. *24*, 89.

HAYAKAWA, K.I. 1978. A critical review of mathematical procedures for determining proper heat-sterilization processes. Food Technol. *32*, 59.

HENDRICKX, M., WENG, Z., MARSMANS, G. and TOBBACK, P. 1992. Validation of time-temperature integrators for thermal processing of foods under pasteurization conditions. Int. J. Food Sci. Technol. *27*, 21.

KIM, H.-J. and TAUB, I.A. 1993. Intrinsic chemical markers for aseptic processing of particulate foods. Food Technol. *47*, 91.

LABUZA, T.P. 1979. A theoretical comparison of losses in foods under fluctuating temperature sequences. J. Food Sci. *44*, 1162.

LABUZA, T.P., 1982. *Shelf-life Dating of Foods*, Food & Nutrition Press, Trumbull, CT.

LABUZA, T.P., 1984. Application of chemical-kinetics to deterioration of foods. J. Chem. Educ. *61*, 348.

LABUZA, T.P. and KAMMAN, J. 1983. Reaction kinetics and accelerated tests simulation as a function of temperature. In *Computer-Aided Techniques in Food Technology*, (I. Saguy, ed.) p. 71, Marcel Dekker, New York.

LUND, D. B. 1975. Heat processing. In *Physical Principles of Food Preservation*, (O. R. Fennema, ed.) Marcel Dekker, New York.
NUNES, R.V., RHIM, W.J. and SWARTZEL, K.R. 1991. Kinetic parameter-evaluation with linearly increasing temperature profiles: integral methods. J. Food Sci. *56*, 1433.
RHIM, J.W., NUNES, R.V., JONES, V.A. and SWARTZEL, K.R. 1989. Determination of kinetic parameters using linearly increasing temperature. J. Food Sci. *54*, 446.
SAPRU, V., TEIXEIRA, A.A., SMERAGE, G.H. and LINDSAY, J.A. 1992. Predicting thermophilic spore population dynamics for UHT sterilization processes. J. Food Sci. *57*, 1248.
SENUM, G.I. and YANG, R.T. 1977. Rational approximations for the integral of the Arrhenius Function. J. Thermal Anal. *11*, 445.
SINGH, R.P. and HELDMAN, D.R. 1984. *Introduction to Food Engineering*, Academic Press, Orlando, FL.
STUMBO, C.R. 1973. *Thermobacteriology in Food Processing*, Academic Press, New York.
SWARTZEL, K.R. 1982. Arrhenius kinetics as applied to product constituent losses in ultra high temperature processing. J. Food Sci. *47*, 1886.
TEIXEIRA, A.A., DIXON, J.R., ZAHRADNIK, J.W. and ZINSMEISTER, G.E. 1969a. Computer determination of spore survival distributions in thermally-processed conduction-heated foods. Food Technol. *23*(3), 78.
TEIXEIRA, A.A., DIXON, J.R., ZAHRADNIK, J.W. and ZINSMEISTER, G. E. 1969b. Computer optimization of nutrient retention in the thermal processing of conduction-heated foods. Food Technol. *23*(3), 137.
TEIXEIRA, A.A., STUMBO, C.R. and ZAHRADNIK, J.W. 1975. Experimental evaluation of mathematical and computer models for thermal process evaluation. J. Food Sci. *40*, 653.
WELLS, J.H. and SINGH, R.P. 1988. A kinetic approach to food quality prediction using full-history time temperature indicators. J. Food Sci. *53*, 1866.

TIME-VARIABLE RETORT TEMPERATURE PROFILES FOR CYLINDRICAL CANS: BATCH PROCESS TIME, ENERGY CONSUMPTION, AND QUALITY RETENTION MODEL[1]

SERGIO F. ALMONACID-MERINO, RICARDO SIMPSON
and J. ANTONIO TORRES

Food Process Engineering Group
Department of Food Science and Technology
Oregon State University
Corvallis, OR 97331-6602

Accepted for Publication May 14, 1993

ABSTRACT

The batch retort model developed uses a heat transfer equation for heat conduction in cylindrical cans, first order kinetics for microbial inactivation, first order kinetics for quality losses and a transient energy balance to estimate steam consumption. For a given retort, lethality process and quality retention, the transient energy balance equation in the model allowed the identification of feasible time-temperature profiles reducing energy consumption, total process time or both. In the examples analyzed and depending upon product specifications, time-variable retort temperatures reduced process time by 18–55 min. These examples suggested that a change from constant to time-variable retort temperatures could increase canning capacity by 20–50%.

INTRODUCTION

The effect of thermal processing on nutrient retention, energy consumption and food safety using constant and time-variable retort temperature (TVRT) can be estimated with computer-supported models (Teixeira *et al.* 1969a,b; Lenz and Lund 1977a,b; Ohlsson 1980a,b; Bhowmik and Hayakawa 1983, 1988; Simpson *et al.* 1989a,b; Banga *et al.* 1991). In the case of conduction-heated foods, the optimum constant retort temperature (CRT) for quality retention and energy consumption do not have to coincide. Although TVRT examples have been included in several studies (Teixeira *et al.* 1975; Saguy and Karel 1979; Nadkarni and Hatton 1985; Banga *et al.* 1991), procedures to verify the feasibility of the selected temperature profile need further analysis. TVRT

[1]OSU Agricultural Experiment Station Publication No. 10,034

profiles for a given retort could be proposed which are feasible only with retort cooling or steam removal devices (Saguy and Karel 1979). The latter situation cannot be detected in predicted energy consumption analyses (Barreiro *et al.* 1984; Bhowmik *et al.* 1985) because they do not include transient energy balance calculations.

An important consideration in canning operations is the varying quantity of available raw materials, which affects the efficient use of canning facilities. After a peak season, the availability of raw materials decreases significantly, reducing the incentive to increase plant capacity. The effect of TVRT on processing time while retaining the safety, quality and energy consumption equivalent to CRT processes needs to be evaluated.

This paper presents a methodology to include a transient energy model to identify feasible TVRT profiles for batch retorts without energy removal devices. The model was used to examine the feasibility of two TVRT profiles assuming a given retort. An optimization technique, the Complex method (Beveridge 1970), was then used to identify feasible TVRT profiles reducing energy consumption, total process time or both while maintaining a specified quality and process lethality. Equivalent lethality processes analyzed include cases where the constant retort temperature for maximum quality retention is lower, equal or higher than the retort temperature for minimum energy consumption.

MATERIALS AND METHODS

Development of Model

A model for commercial sterilization was developed by examining the following phenomena and their governing equations. The unsteady state conduction heat transfer with thermophysical properties independent of temperature can be described as,

$$\frac{1}{\alpha}\frac{\partial T}{\partial \theta} = \frac{1}{r}\frac{\partial T}{\partial r} + \frac{\partial^2 T}{\partial r^2} + \frac{\partial^2 T}{\partial z^2} \tag{1}$$

with the following boundary conditions:

$$T_{can\ surface,\ heating} = RT(\theta)$$

$$T_{can\ surface,\ cooling} = TW(\theta)$$

The kinetics of cell destruction was quantified as,

$$\frac{dN}{d\theta} = -k_m N \tag{2}$$

with

$$k_m = \frac{\ln 10}{D_m}$$

Quality losses were assumed to follow first-order kinetics:

$$\frac{dC}{d\theta} = -k_c C$$

with

$$k_c = \frac{\ln 10}{D_c} \tag{3}$$

The transient energy balance for a system defined as the retort, cans without their contents, and the steam and condensate in the retort requires no work term. The heat transfer terms include radiation and convection to the plant environment, and heat transfer to the food in the can. Therefore,

$$[\sum_{i=1}^{n} m'_i \hat{H}_i]_{input} - [\sum_{j=1}^{m} m'_j \hat{H}_j]_{output} + \sum_{i=1}^{p} Q'_i = [\frac{d(\hat{E}M)}{d\theta}]_{system} \tag{4}$$

The previous equations were solved simultaneously using an explicit finite difference method with a time increment of 7.5 s (Teixeira *et al.* 1969b). Microbial lethality, quality retention and energy consumption were calculated with kinetic constants evaluated using an average temperature during the time interval. The final expression for microbial lethality is then,

$$N_{(r,z)}^{\theta+\Delta\theta} = N_{(r,z)}^{\theta} \, EXP\{\frac{-\ln 10}{D_{m,R}\, 10^{\frac{T_R - T_{(r,z)}}{z_m}}} \Delta\theta\} \tag{5}$$

with

$$D_m = D_{m,R}\, 10^{\frac{T_R - T_{(r,z)}}{z_m}}$$

and the analogous expression for quality losses is,

$$C^{\theta+\Delta\theta}_{(r,\,z)} = C^{\theta}_{(r,\,z)}\ EXP\{\frac{-\ln 10}{D_{c,R}\ 10^{\frac{T_R - T_{(r,\,z)}}{z_c}}}\Delta\theta\} \tag{6}$$

with

$$D_c = D_{c,R}\ 10^{\frac{T_R - T_{(r,\,z)}}{z_c}}$$

The transient energy balance was solved as follows:

$$(m'_j\ \hat{H}_j)_{in} - (m'_i\ \hat{H}_i)_{out} + Q'_r + Q'_c + Q'_p = \frac{d\ (\hat{E}M)}{d\theta}_{system} \tag{7}$$

where

$$\frac{d(\hat{E}M)}{d\theta}_{system} = \frac{d(\hat{E}_1\ M_1)}{d\theta} + \frac{d(\hat{E}_2\ M_2)}{d\theta} + \frac{d(\hat{E}_3\ M_3)}{d\theta} \tag{8}$$

The steam consumption during each time interval (7.5 s) can be calculated using average properties as follows:

$$m_{steam} = (m'_{in})\Delta\theta =$$

$$\frac{\Delta\hat{E}_1M_1 + \Delta\hat{E}_2M_2 + \Delta\hat{E}_3M_3 - \int_{\theta}^{\theta+\Delta\theta} Q_r d\theta - \int_{\theta}^{\theta+\Delta\theta} Q_c d\theta - \int_{\theta}^{\theta+\Delta\theta} Q_p d\theta + (m'\hat{H}_{average})_{out}\ \Delta\theta}{(\hat{H}_{average})_{in}} \tag{9}$$

Correlations valid in the range of interest (105–135C), were used to estimate the thermodynamic properties of steam and condensed water. Steam removed by bleeding was calculated using the procedures described by Barreiro *et al.* (1984). The energy consumed during the venting time, a constant value for a given retort, was not needed for the purposes of this study. The characteristics of the retort and canned products assumed in these calculations (see Appendix) were obtained from Barreiro *et al.* (1984). An exception were the European style 73 × 31 mm cans (Ohlsson 1980a,b) used in our simulations instead of the 307 × 409 cans used by these authors. The latter size was used only in preliminary model verifications by comparing our calculations with values published by Barreiro *et al.* (1984).

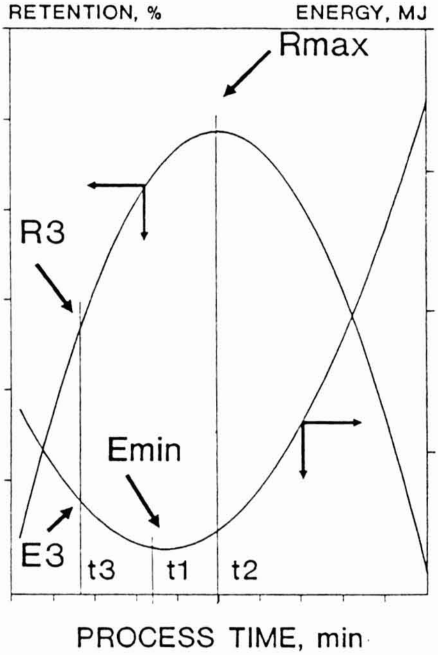

FIG. 1. SCHEMATIC REPRESENTATION OF QUALITY RETENTION AND ENERGY CONSUMPTION FOR EQUIVALENT LETHALITY PROCESSES

Process Time

An expected benefit of TVRT processes is the reduction of process time while retaining quality and energy use levels similar or better to equivalent-lethality processes at constant temperature. If the number of cans processed per year (N_t) is related to process time (t_p), a simple procedure to quantify the impact on production capacity, achieved by reducing process time, can be derived as follows:

$$N_t = n\, N_b \tag{10}$$

$$N_b = \frac{T_y}{t_T} \tag{11}$$

From Eq. (10–11):

$$N_t = \frac{n\, T_y}{t_T} \tag{12}$$

where

$$t_T = t_x + t_p \tag{13}$$

Therefore,

$$N_t = \frac{n\ T_y}{t_x + t_p} \tag{14}$$

Taking derivatives and rearranging Eq. (14) yields,

$$\frac{dN_t}{N_t} = \frac{-t_p}{t_x + t_p}\left(\frac{dt_p}{t_p}\right) \tag{15}$$

$$\frac{\Delta N_t}{N_t} \approx \frac{-t_p}{t_x + t_p}\left(\frac{\Delta t_p}{t_p}\right) \tag{16}$$

which quantifies changes in plant production capacity for a given process time change.

Process Improvement: Search Method

The simultaneous search to improve quality, reduce energy consumption and process time for a given retort (see Appendix) was accomplished as follows (Fig. 1). The procedure required to find first two equivalent lethality processes at constant temperature maximizing quality and minimizing energy consumption, respectively (Simpson *et al.* 1989a,b). The best process at constant temperature from an energy consumption point of view (energy consumption Emin) was defined as retort temperature T1 and process time t1. The best process at constant temperature from a quality point of view (quality retention Rmax) was defined as retort temperature T2 and process time t2. A search was then conducted to find a feasible time-temperature profile minimizing process time, retaining the same or higher quality, and consuming the same or less energy than the best constant temperature processes. Using the Complex method (Beveridge 1970), this search was accomplished by finding first a feasible TVRT profile with a process time tl maximizing quality retention while keeping Emin as a search constraint. The search was stopped when a process with the specified energy consumption (Emin) and process time (tl) as well as having a quality retention higher or equal to Rmax, was found. The procedure continued by searching for

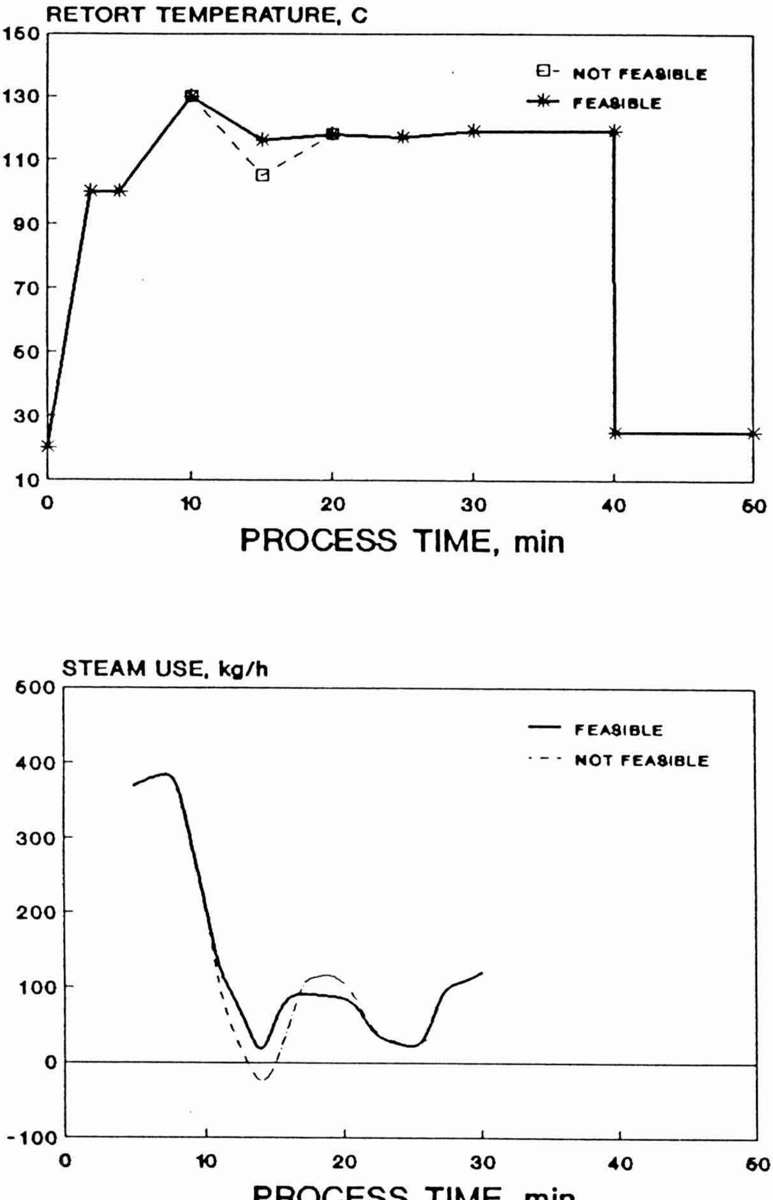

FIG. 2. TIME-VARIABLE RETORT TEMPERATURE (TVRT) PROCESSING, EXAMPLE 1
a. TVRT profiles; b. predicted steam consumption.

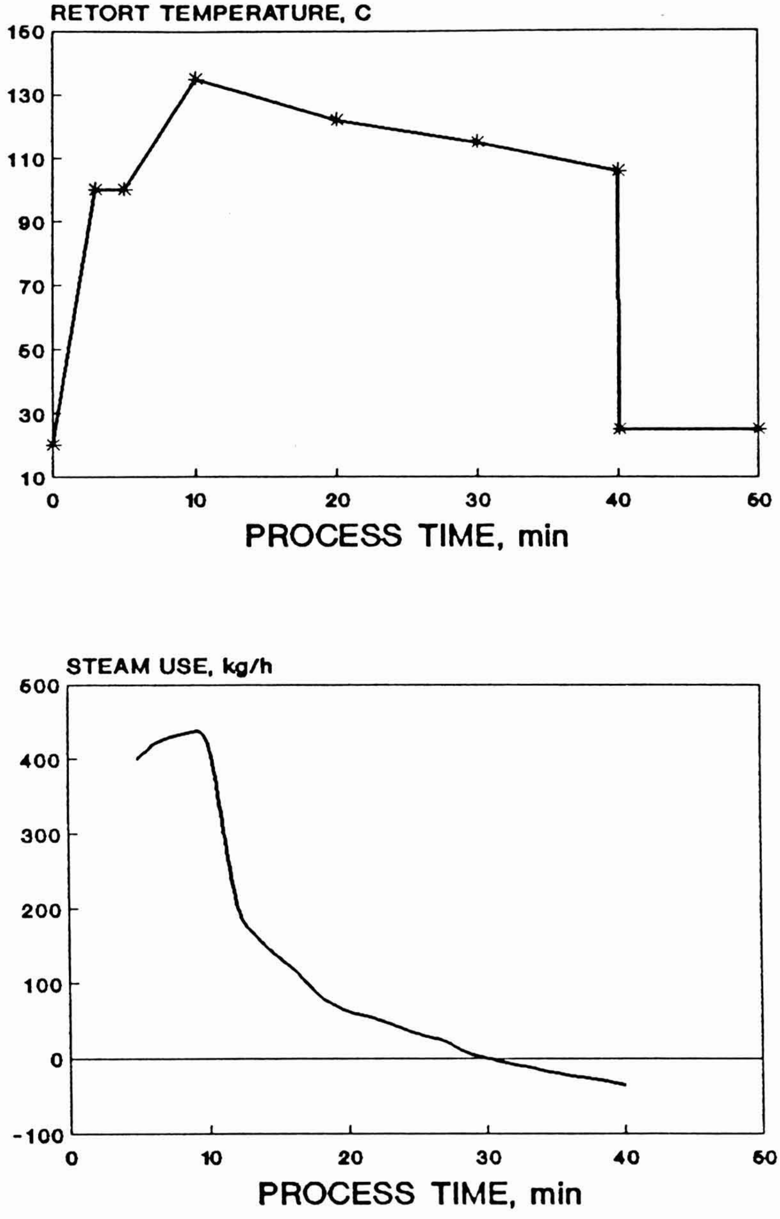

FIG. 3. TIME-VARIABLE RETORT TEMPERATURE (TVRT) PROCESSING, EXAMPLE 2
a. TVRT profile; b. predicted steam consumption.

a process with retention Rmax and energy consumption Emin but now with t3 (t3 < tl) as process time. The t3 min process at constant temperature had a quality retention R3 < Rmax and an energy consumption E3 > Emin (Fig. 1). The program was run with energy consumption (E3) as a constraint and used to maximize quality retention. The program was stopped when it found a feasible process with R2 > Rmax and E < E3. Next, quality retention was used as a constraint (R2 > Rmax) to minimize energy consumption. The program was stopped when R > Rmax and E < Emin with t3 min as a process time. The search was continued by repeating the above procedure for shorter process times.

RESULTS AND DISCUSSION

Identification of Feasible TVRT Profiles

A TVRT profile was selected to highlight the advantage of a model incorporating a transient energy balance equation (Fig. 2a). The process chosen was not feasible without an energy removal device as indicated by negative steam consumption during the time period between 13 and 16 min (Fig. 2b). In other words, the operation of the assumed retort for the TVRT profile specified would require not only closing the steam valve but also eliminating heat by steam removal beyond the amount removed by bleeding, or by using a cooling device.

The computer-implemented model was also used to find which temperature at 15 min would ensure no negative steam consumption. In the original TVRT profile, the temperature dropped from 130C at 10 min to 105C at 15 min. The temperature at 15 min should be no lower than 116C (Fig. 2a) to avoid a negative steam consumption situation (Fig. 2b).

A TVRT profile (Fig. 3a) with values similar to those published by Teixeira *et al.* (1975) was examined to determine if it represented a case of negative steam consumption for the retort assumed in this study (see Appendix). Steam consumption after 10 min of retort operation showed a negative steam consumption during the 30–40 min time interval (Fig. 3b). It is important to highlight that steam consumption depends not only on the time-temperature profile but also on the characteristics of the food product, the retort used (size, heat irradiation coefficient, etc.) and the processing environment.

Process Improvement

The effect on the retention of three quality factors, and the corresponding energy consumption of equivalent lethality processes at constant retort temperature are shown in Fig. 4. A particular case occurs when z_c = 25C,

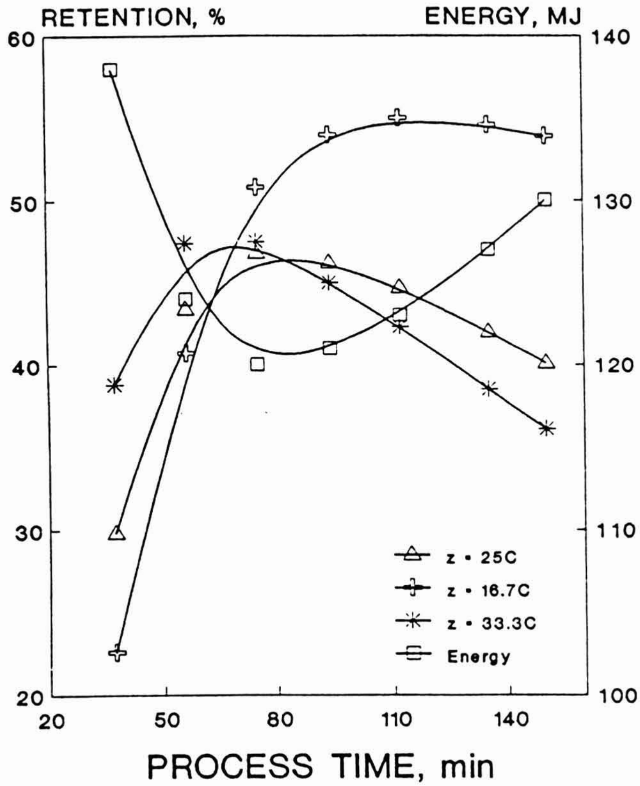

FIG. 4. QUALITY RETENTION AND ENERGY CONSUMPTION FOR EQUIVALENT LETHALITY PROCESSES

because the retort temperature maximizing quality retention (46.8% at 122.2C, 75 min heating time) also minimizes energy consumption (1.2×10^8 J). In this case, the search procedure identified a 70 min TVRT process with the same energy consumption and quality retention (Table 1). An attempt to further reduce the process time identified a 56 min TVRT process (Fig. 5) with the same energy consumption but with a slightly lower nutrient retention, 44.2% instead of 46.8% (Table 1). The slight difference in nutrient retention (2.6%) might be commercially acceptable in view of the 20% reduction in process time (14 min).

A more general process situation results when z_c = 16.7C (Fig. 4). The constant retort temperature that maximizes quality retention is different from the temperature that minimizes energy consumption. The search procedure was started with a CRT process at 122.2C (Table 1). It was not possible to find a 75 min feasible TVRT process consuming 1.2 × 108 J (Emin) and yielding a

55% quality retention (Rmax). The search gave the following results, an energy consumption of 1.2×10^8 J and a 51.3% quality retention (Table 1).

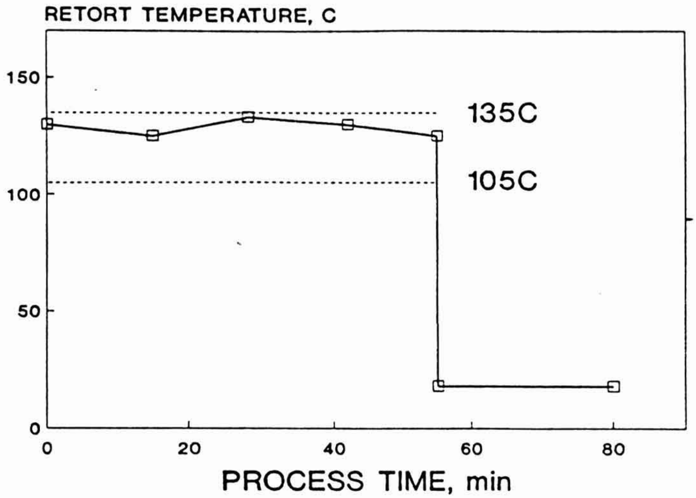

FIG. 5. TIME VARIABLE RETORT TEMPERATURE (TVRT) PROFILE IMPROVING ENERGY CONSUMPTION AND QUALITY RETENTION
(z_c = 25C, $D_{c,\,121.1C}$ = 188.7 min)

Nevertheless, the effort to reduce process time was continued. The search for a t3 = 56 min TVRT profile resulted again in the same energy consumption, but the quality retention was only 41.3%.

The example with z_c = 33.3C is analogous to the case with z_c = 16.7C (Fig. 4). In this case TVRT reduced process time from 75 to 56 min while retaining the minimum energy consumption and maximum quality retention of the CRT processes (Table 1).

Process Time

A significant advantage of TVRT profiles is the reduction in process time while maintaining an energy consumption and quality similar to those possible with CRT. To quantify this effect on plant production capacity, the process time and data reported in Table 1 were evaluated using Eq. (16) assuming the time required for preparing, loading and unloading the retort is 30 min total. In case 1 (Table 1), the processing times were 75 min for a CRT at 122.2C and 56 min for a TVRT profile, therefore,

$$\frac{\Delta N_t}{N_t} \approx -\frac{75}{(75 + 30)} \frac{(-19)}{75} \approx 0.18$$

i.e., plant production capacity would increase 18%. In case 2a (Table 1), the processing times were 112 min for a CRT at 116.3C and 56 min for a TVRT profile, therefore

$$\frac{\Delta N_t}{N_t} \approx -\frac{112}{(112 + 30)} \frac{(-56)}{112} \approx 0.39$$

In this case plant production capacity would increase almost 40%. Calculations for other t_x values show TVRT processes could increase plant capacity 20–50% (Table 2).

TABLE 1.
THERMAL PROCESS IMPROVEMENT SEARCH[1]
(F_o = 15 min, z_m = 10 C, $D_{m,r}$ = 3 min, T_r = 121.1C)

TEMPERATURE	TIME	%RETENTION	ENERGY, Jx10^{-8}
CASE 1: Retort temperature and processing time for minimum energy consumption and maximum quality retention coincide			
z_c = 25 C, $D_{c,\ 121.1\ C}$ = 188.7 min			
CRT, 122.2 C	75	46.8	1.20
TVRT, 110-135 C	70	46.8	1.20
TVRT, 110-135 C	56	44.2	1.20
CASE 2: Retort temperature and processing time for minimum energy consumption and maximum quality retention do not coincide			
a. z_c = 16.7 C, $D_{c,\ 121.1\ C}$ = 202 min			
CRT, 116.3 C	112	55.0	1.23
CRT, 122.2 C	75	50.8	1.20
TVRT, 110-135 C	75	51.3	1.20
TVRT, 110-135 C	56	41.3	1.20
b. z_c = 33.3 C, $D_{c,\ 121.1\ C}$ = 202 min			
CRT, 122.2 C	75	47.5	1.20
TVRT, 110-135 C	56	48.1	1.20

(1) CRT = constant retort temperature, TVRT = time-variable retort temperature

TABLE 2.
PLANT PRODUCTION CAPACITY INCREASE
ACHIEVED BY TVRT PROCESSES[1]

	Cases considered (2)		
t_x, min	Case 1	Case 2a	Case 2b
10	22%	46%	22%
30	18%	39%	18%
40	17%	37%	17%
60	15%	33%	15%

(1) TVRT = time-variable retort temperature.

(2) See Table 1 for further details.

CONCLUSIONS

The incorporation of transient energy calculations in a batch retort model allows to identify which TVRT profiles can be used without retort modifications. Combining the above procedure and the Complex method, TVRT profiles were identified to reduce process time by 18–55 min depending upon product and process specifications. The methodology was particularly useful to analyze equivalent-lethality processes when the constant retort temperatures for maximum quality retention and minimum energy consumption do not coincide.

The opportunity to find TVRT processes with the maximum quality retention and minimum energy consumption possible for CRT processes but using less process time could increase the processing capacity of a given plant an estimated 20–50%. The implementation of TVRT profiles could be facilitated by the development of on-line computer control programs (Simpson *et al.* 1992). Automatic control is needed to minimize differences between the actual and the specified TVRT process. Finally, the energy consumption profiles obtained by transient energy calculations could be used to optimize the scheduling of retort operations and thus maximize the use of installed boiler capacity. Improved scheduling could also reduce the frequency of process deviations.

ACKNOWLEDGMENTS

The authors gratefully acknowledge the contribution of Ms. Silvana Roncagliolo whose computer programming skills were essential for the completion of this project. This publication is the result of research sponsored in part by Oregon Sea Grant with funds from the National Oceanic and Atmospheric Administration, Office of Sea Grant, Department of Commerce, under grant no. NA85AA-D-SG095 (project no. E/ISG-6) and from appropriations made by the Oregon State Legislature.

NOMENCLATURE

C	Concentration of quality factor (nutrient, color, etc.) at any time θ
$D_{c,r}$	Chemical decimal reduction time at temperature $T = T_R$, min
D_c	Quality decimal reduction time at temperature T, min
$D_{m,r}$	Microbial decimal reduction time at temperature $T = T_R$, min
D_m	Microbial decimal reduction time at temperature T, min
$\hat{E}$	Specific energy of total system, J/kg
$\hat{E}$	Specific energy of steam inside autoclave, J/kg
$\hat{E}2$	Specific energy of condensed steam inside autoclave, J/kg
$\hat{E}3$	Specific energy of autoclave, basket and tin cans, J/kg
F_o	Process lethality, min
$\hat{H}_{i,in}$	Enthalpy input, J/kg, stream i, i = 1, 2, ..., n
$\hat{H}_{j,out}$	Enthalpy output, J/kg, stream j, j = 1, 2, ..., m
k	Rate constant at temperature T, s^{-1}
kc	First-order rate constant for quality loss, s^{-1}
km	First-order rate constant for microbial inactivation, s^{-1}
M	Mass of total system, kg
M_1	Steam mass inside autoclave, kg
M_2	Condensed steam mass inside autoclave, kg
M_3	Mass of autoclave, basket and tin cans, kg
$m_{i,in}$	Mass flow rate input, kg/s, stream i, i = 1, 2, ..., n
$m_{j,out}$	Mass flow rate output, kg/s stream j, j = 1, 2, ..., m
M_{system}	Total mass of the system, kg
n	Number of cans per batch
N	Microbial load, CFU/kg
N_b	Number of batches per year
N_t	Number of cans processed per year
Q'_c	Heat lost by convection, J/s
Q'_i	Heat term, J/s, stream i, i = 1,2, .., p
Q'_p	Heat transfer with the product in the can, J/s

Q'_r	Heat lost by radiation, J/s
r	Cylindrical coordinate, radial direction
R	Universal gas constant, J/mol K
RT	Retort temperature, C
$T_{(r,z)}$	Temperature at any point and time θ, C
T_c	Can center temperature, C
T_i	Initial temperature, C
t_p	Process time, min
T_R	Reference temperature, C
t_T	Batch time, min
t_x	Total time to prepare and discharge the retort, min
T_y	Plant operation time per year, h
WT	Cooling water temperature, C
z	Cylindrical coordinate, vertical direction
z_c	Slope index of quality factor destruction rate curve, C
z_m	Slope index of microbial death time curve, C
α	Thermal diffusivity, m^2/s
θ	Time, s

APPENDIX: Processing Conditions for Computer Simulation Model

Retort	Mass, 163.6 kg Area, 2.97 m^2 Volume, 0.356 m^3 c_p, 0.5 kJ/kg C Bleeder area, 7.94 x 10^{-6} m^2
Lethality	T_R, 121C $D_{m,R}$, 3 min z_m, 10C
Product	Thermal diffusivity, 1.6 x 10^{-7} m^2/s cp, 3.8 kJ/kg C density, 1,100 kg/m^3
Operation conditions	Initial retort temperature (T_i), 20C Initial product temperature, 71.1C Environmental temperature, 30C Process temperature, variable European can, 73 x 31mm Can mass, 0.0112 kg/can

Number of cans in load, 950 cans/batch
F_o, 15 min
Time-temperature profile limits, 110-135C

REFERENCES

BANGA, J.R., PEREZ-MARTIN, R.I., GALLARDO, J.M. and CASARES, J.J. 1991. Optimization of the thermal processing of conduction-heated canned foods: study of several objective functions. J. Food Eng. *14*, 25–51.

BARREIRO, J.A., PEREZ, C.R. and GUANIQUATA, C. 1984. Optimization of energy consumption during the heat processing of canned foods. J. Food Eng. *3*(1), 27–37.

BEVERIDGE, G.S.G. and SCHECHTER, R.S. 1970. *Optimization: Theory and Practice*, McGraw Hill, New York.

BHOWMIK S.R. and HAYAKAWA, K.I. 1983. Influence of selected thermal processing conditions on steam consumption and on mass average sterilizing values. J. Food Sci. *48*, 212–216, 225.

BHOWMIK, S.R. and HAYAKAWA, K.I. 1988. Quality retention and steam consumption of selected thermal processes. Lebensm. Technol. *21*(1), 13–19.

BHOWMIK S.R., VISCHENEVETSKY, R. and HAYAKAWA, K 1985. Mathematical model to estimate steam consumption in thermal processing of canned food by a vertical still retort. Lebensm. Technol. *18*(1), 15-23.

LENZ, M.K. and LUND, D.B. 1977a. The lethality-Fourier number method: experimental verification of a model for calculating temperature profiles and lethality in conduction-heating canned foods. J. Food Sci. *42*(4), 989-996, 1001.

LENZ, M.K. and LUND, D.B. 1977b. The lethality-Fourier number method: experimental verification of a model for calculating average quality factor retention in conduction-heating canned foods. J. Food Sci. *42*(4), 997-1001.

NADKARNI, M.M. and HATTON, T.A. 1985. Optimal nutrient retention during the thermal processing of conduction-heated canned foods: application of the distributed minimum principle. J. Food Sci. *50*, 1312-1321.

OHLSSON, T. 1980a. Optimal sterilization temperatures for flat containers. J. Food Sci. *45*, 848-852.

OHLSSON, T. 1980b. Optimal sterilization temperatures for sensory quality in cylindrical containers. J. Food Sci. *45*, 1517-1521.

SAGUY, I. and KAREL, M. 1979. Optimal retort temperature profile in optimizing thiamine retention in conduction type heating of canned food. J. Food Sci. *44*, 1485-1490.

SIMPSON, R., ALMONACID-MERINO, S.F. and TORRES, J.A. 1993. Mathematical models and logic for the computer control of batch retort process operations: conduction-heated foods. J. Food Eng. *20*, 283–295.

SIMPSON, R., ARIS, I. and TORRES, J.A. 1989a. Retort processing operations: conduction-heated foods in oval-shaped containers. OSU Sea Grant Techn. Rep. ORESU-T-89-002, 20 pp.

SIMPSON, R., ARIS, I. and TORRES, J.A. 1989b. Evaluation of the sterilization process for conduction-heated foods in oval-shaped containers. J. Food Sci. *54*, 1327-1332, 1363.

TEIXEIRA, A.A., DIXON, J.R., ZAHRADNIK, J.W. and ZINSMEISTER, G.E. 1969a. Computer determination of spore survival distributions in thermally-processed conduction-heated foods. Food Technol. *23*, 78-80.

TEIXEIRA, A.A., DIXON, J.R., ZAHRADNIK, J.W. and ZINSMEISTER, G.E. 1969b. Computer optimization of nutrient retention in the thermal processing of conduction-heated foods. Food Technol. *23*, 845-850.

TEIXEIRA, A.A., ZINSMEISTER, G.E. and ZAHRADNIK, J.W. 1975. Computer simulation of variable retort control container geometry as a possible means of improving thiamine retention in thermally processed foods. J. Food Sci. *40*, 656-659.

INFLUENCE OF RHEOLOGICAL PROPERTIES OF FLUID AND SEMISOLID FOODS ON THE PERFORMANCE OF A FILLER

M.A. RAO and H.J. COOLEY

Department of Food Science and Technology
Cornell University-Geneva
Geneva, NY 14456

and

C. ORTLOFF, K. CHUNG and STAN C. WIJTS

CTC and FMC-Food Processing Systems
317 Brokaw Road, Suite A
Santa Clara, CA 95050

Accepted for Publication May 14, 1993

ABSTRACT

For low-viscosity foods, in a piston filler (FMC PN010), power-law relationships were found between the number of cycles/minute at which splashing occurred on the rim of a container versus viscosities of the test fluids. Splashing was due to either the breakup of a discharge jet in the nozzle or overflow of discharge fluid over the rim of a container. The formation of droplets due to breakup of discharge jets was confirmed by solution of the flow equations on a Cray-2 super computer. With foods containing particulates in a low-viscosity liquid, splashing occurred when the food hit the bottom of the container and again when the plunger hit the top of the heaped food. With foods having high magnitudes of yield stresses, the plug formed in the discharge nozzle of the filler contributed to heaping of the foods.

INTRODUCTION

Rheological behavior plays an important role in the handling of foods (Rao and Anantheswaran 1982). Filling of containers with foods is an essential unit operation in food processing. Filling speeds can range from a few to several hundred containers per minute. The rheological characteristics of a food can cause splashing and heaping that in turn prevent adequate closure of the container and result in economic losses. For example, splashed or spread food on the rim of a microwaveable container may impede adequate closure. The objective of the present study was to study experimentally and theoretically the role of rheological properties on the performance of a FMC model PN010 filler. Specifically, the phenomenon associated with the discharge of food from the nozzle of a filler needs to be understood. Because of the presence of a free surface at the nozzle discharge end, the studied problem is different than flows in enclosed systems, such as periodic flow in a pipe.

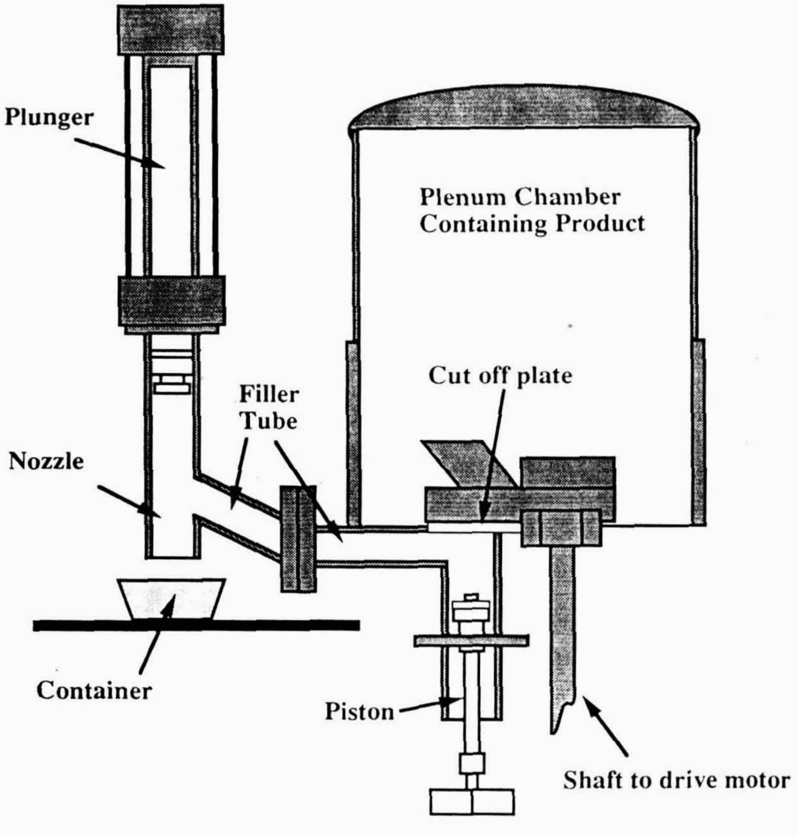

FIG. 1. SCHEMATIC OF FMC PN010 FILLER

MATERIALS AND METHODS

Filler

A schematic diagram of the PN010 filler is shown in Fig. 1. Food stored in a chamber is first drawn and later pushed into a filler tube-nozzle (3.81 cm dia) assembly, and finally discharged into a container by a plunger. The volume of food and the rate of discharge could be adjusted. The discharge of foods with different rheological properties and at different discharge rates was studied.

Fluids Studied Experimentally

Experimental studies on the filler were conducted with both Newtonian fluids: water, concentrated apple juice (51 and 70 °Brix), and vegetable oil, as

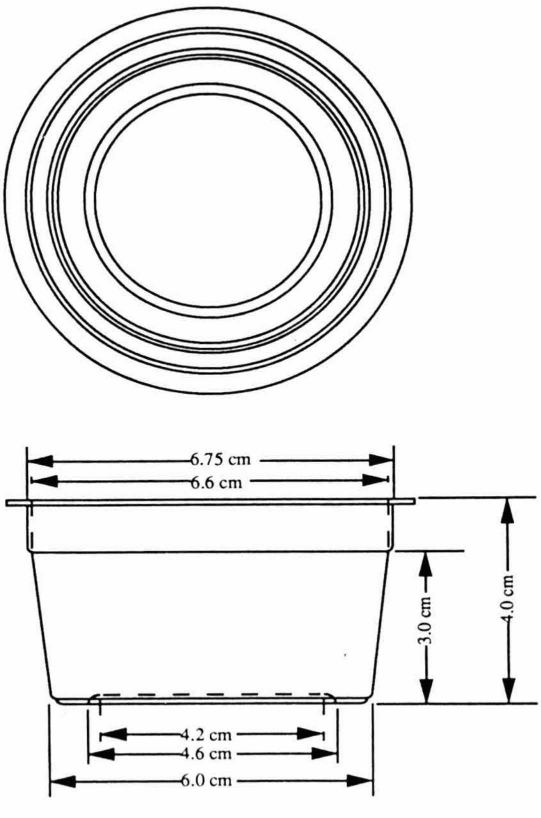

FIG. 2. SCHEMATIC AND DIMENSIONS OF SMALL CUP, 82 ml VOLUME

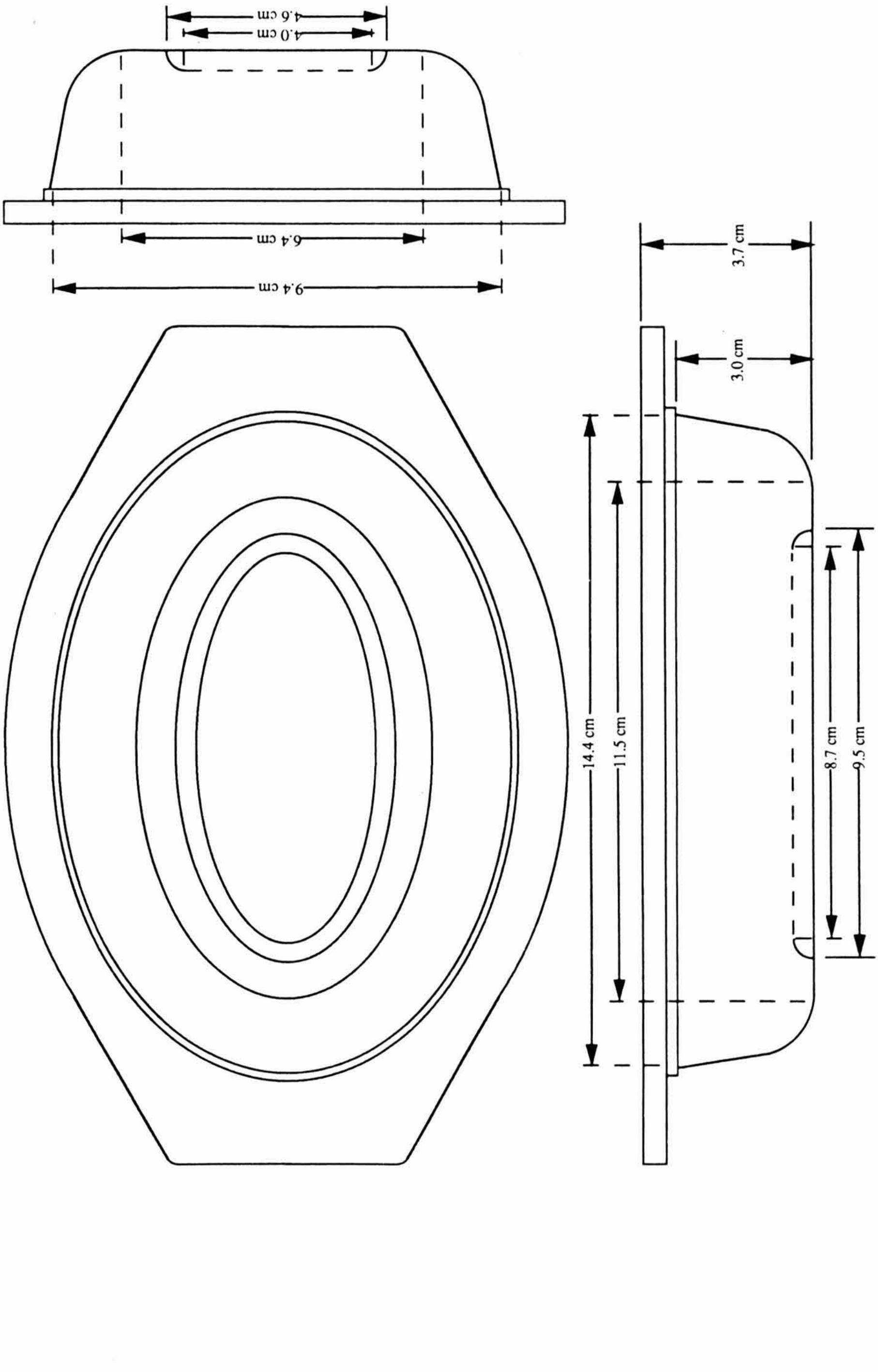

FIG. 3. SCHEMATIC AND DIMENSIONS OF SMALL OVAL CONTAINER, 218 ml VOLUME

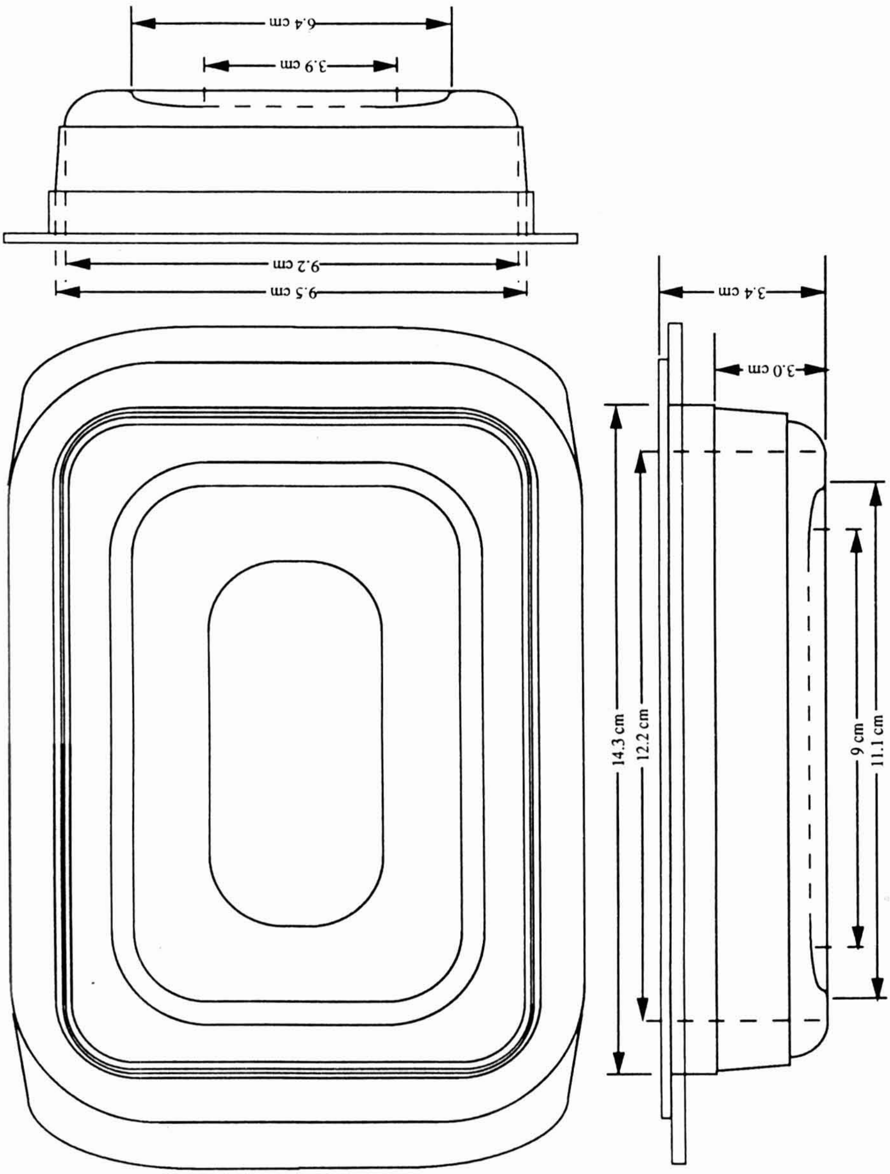

FIG. 4. SCHEMATIC AND DIMENSIONS OF LARGE OVAL CONTAINER, 295 ml VOLUME

non-Newtonian fluid and semisolid foods: apple sauce, tomato concentrates, pet food, pork and beans, and crushed pineapple. The filler was operated such that it delivered a food sample into three containers: a small cup 82 ml (5 in^3), a small oval container 218 ml (13.3 in^3), and a large oval container 295 ml (18 in^3), at 24-36, 13-26, and 11-29 cycles/min (CPM) for the three containers, respectively. The dimensions of the three containers are shown in Figures 2–4. The rheological properties (shear rate-shear stress and, where applicable, yield stress) of the test foods without particulates were determined at the fill temperature with either a Haake RV2 (Fison Instruments, Saddlebrook, NJ) or a Deer Rheometer III (Deer Rheometer Inc., Niewleusen, The Netherlands). The properties of foods with particulates were determined with a mixer paddle attached to the Haake RV2 viscometer to obtain RPM-torque data on a standard fluid (y) and a test substance (x) placed in a jacketed vessel; theRPM-torque data were converted to shear rate-shear stress data (Rao 1975). The power law (Eq. 1) and the Casson (Eq. 2) models were used to fit the rheological data.

$$\sigma = K\dot{\gamma}^{n} \quad (1)$$

$$\sigma^{0.5} = K_{oc} + K_c\dot{\gamma}^{0.5} \quad (2)$$

where σ is the shear stress (Pa), $\dot{\gamma}$ is the shear rate (s^{-1}), K is the consistency index ($Pa.s^n$), n is the flow behavior index (dimensionless), and $K_{oc}2$ is the Casson yield stress (Pa), and K_c^2 is the Casson viscosity (Pa.s). The power law model was used because it is extensively used in practical applications, and the Casson model was used because it is easy to use and provides reasonable estimates of yield stress.

Computer Simulation

The transient flow was also studied by solving the pertinent flow equations using the FLOW-3D CFD code on a Cray-2 super computer. The code is based on the MAC finite difference scheme and incorporates the effects of turbulence, viscosity, wall shear, surface tension, and free surface effects on transient flow behavior (Hirt and Sicilian 1985; Hirt and Nichols 1981; Harlow and Welch 1965; Welch *et al.* 1965). A transient input mass flow distribution was determined corresponding to the material displaced by the plunger acting on a stationary mass in the filler tube. The additional mass input causes product fragmentation due to splashing against the side wall and consequent breakup; spalled fluid droplets then undergo ballistic free flight and recombination in container. The adherence of product droplets and subsequent motion along the vertical nozzle wall results from a combination of gravity, surface tension, and wall shear effects. Simulation of the plunger action was obtained by launching

TABLE 1.
RHEOLOGICAL DATA ON THE TEST FLUIDS[a]

Test Fluid	Temperature (C)	K or η ($Pa.s^n$)	n (-)	σ_{0C} (Pa)
Water[b]	38	$7.78x10^{-4}$	1.0	NA
Corn oil	32	0.023	1.0	NA
Corn oil	36	0.017	1.0	NA
Corn oil	41	0.015	1.0	NA
Apple juice 69.8 °Brix	25	0.243	1.0	NA
Apple juice 65.3 °Brix	23	0.093	1.0	NA
Apple juice 69.8 °Brix	43	0.028	1.0	NA
Apple juice 51.1 °Brix	25	0.019	1.0	NA
Guar gum 0.5% (w/v)	25	0.518	0.55	NA
Guar gum 0.3% (w/v)	23	0.072	0.72	NA
Guar gum 0.75% (w/v)	21	2.95	0.44	NA
Guar gum 1.0% (w/v)	21	8.70	0.41	NA
Tomato paste 29.7 °Brix	32	208	0.27	206
Tomato paste 29.7 °Brix	39	179	0.31	180
Tomato puree 23.8 °Brix	33	48	0.47	40
Tomato puree 23.8 °Brix	39	34	0.52	29
Tomato puree 16.3 °Brix	25	24	0.23	38
Pork and beans	32	117	0.90	6.9
Pork and beans	38	106	0.92	3.6
Apple sauce	32	200	0.42	240
Crushed pineapple	17	15.2	0.80	11.8
Dog food-A (diluted)[c]	19	863	0.23	659
Dog food-B (diluted)[d]	19	776	0.16	630

[a]K is consistency index and η is viscosity of food in Pa.s units; σ_{0C} is the yield stress in Pa--NA indicates not applicable due to negligible magnitudes.
[b]Viscosity of water was taken from the Handbook of Chemistry and Physics
[c]Dog food diluted with water; data were obtained with a six-blade paddle--4 cm in diameter.
[d]Dog food diluted with water; data were obtained with a four-blade paddle--3.1 cm in diameter.

a plug of residual food product adhering to the nozzle walls into a nearly full container. The terminal velocity of the plunger was used as the launch speed. A typical run simulating flow in 1 s took about 10 h of computation time on a Cray-2 super computer.

RESULTS AND DISCUSSION

Magnitudes of rheological properties of models fluids and foods are summarized in Table 1.

Discharge Jet(s)

As a general observation, with high viscosity fluids such as a 69.8°Brix concentrated apple juice sample and a 0.5 % guar gum solution, a single discharge jet located close to the axis of the discharge nozzle was observed. In contrast, with low viscosity fluids, such as water and 51.2 °Brix apple juice, usually there were two or three jets—one or two much smaller than the other(s); further, the large jet discharged not from an axisymmetric position, but from the portion of the nozzle wall that was either close to the reservoir or away from the reservoir. The skewed discharge often resulted in the food being washed over the side of the container. Splashing also occurred when a big jet impinged on the surface of the liquid already in the container.

Effect of Viscosity on Splashing/Overflow

The CPM at which splashing or overflow first occurred versus viscosity of Newtonian liquids for the small cup (82 ml), a small oval container (218 ml), and a large oval container (295 ml) are shown in Fig. 5, 6, and 7, respectively. A power law relationship was found between CPM at splash and viscosity for the three containers. These figures are useful in practice in that CPM values that lie above the curves will not be acceptable because of splashing or overflow. The figures are examples of the need to know the magnitudes of viscosity of foods in fundamental units such as poise or Pa.s, instead of consistencies obtained with quality control instruments.

Depending on the magnitude of viscosity, it appears that one or two mechanisms contributed to the splashing phenomena: (1) overflow over the rim of low-viscosity foods discharged at high velocities, and (2) break up of fluids into droplets that land on the rim of a container. The former occurred with low-viscosity foods (Tl less than about 0.1 Pa.s) and can be eliminated by reducing the fluid discharge velocities. Assuming an average velocity of the fluid during the discharge cycle and using properties of Newtonian fluids, one can calculate the critical Reynolds numbers corresponding to the splash-no splash boundaries (Figs. 5–7). For example, for filling the 295 ml container with water, the critical flow Reynolds number is about 3,500. However, the break up of fluid in to droplets is a complex phenomenon that could not be explained in terms of a critical Reynolds numbers. For example, for fluids with viscosity from 0.1 to 0.6 Pa.s, the calculated critical Reynolds numbers were much lower in magnitude, about 8 to 38. Therefore, a careful numerical study of the discharge jets was necessary.

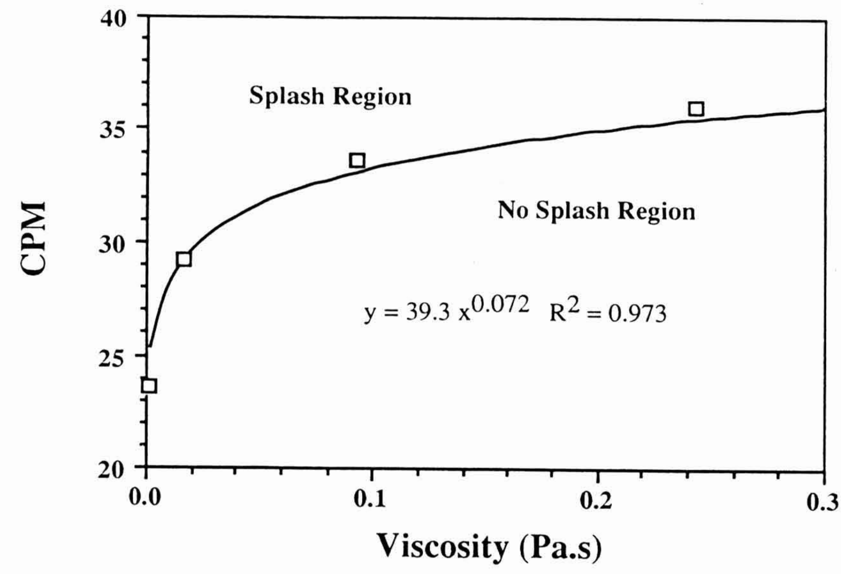

FIG. 5. VISCOSITY (Pa.s) OF NEWTONIAN FLUIDS VERSUS CYCLES/MIN (CPM) AT SPLASH FOR 82 ml CUP

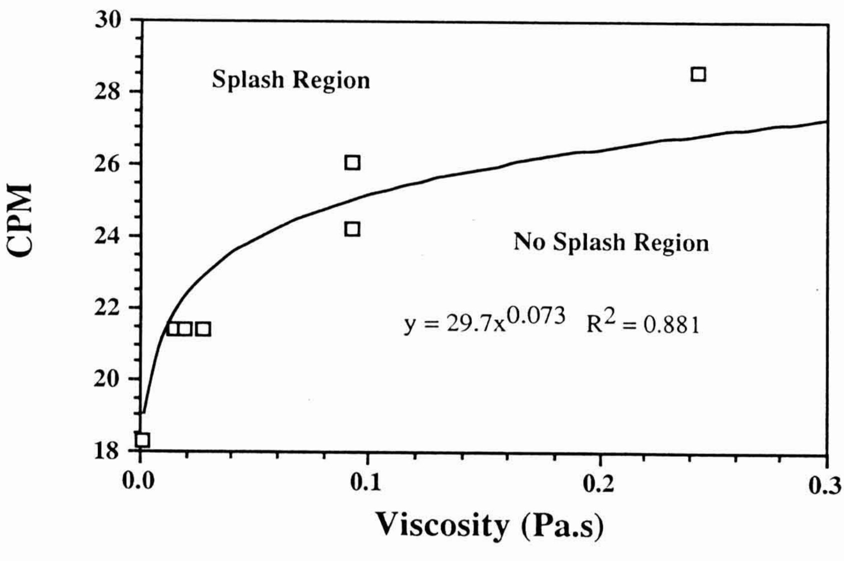

FIG. 6. VISCOSITY (Pa.s) OF NEWTONIAN FLUIDS VERSUS CYCLES/MIN (CPM) AT SPLASH FOR 218 ml OVAL CONTAINER

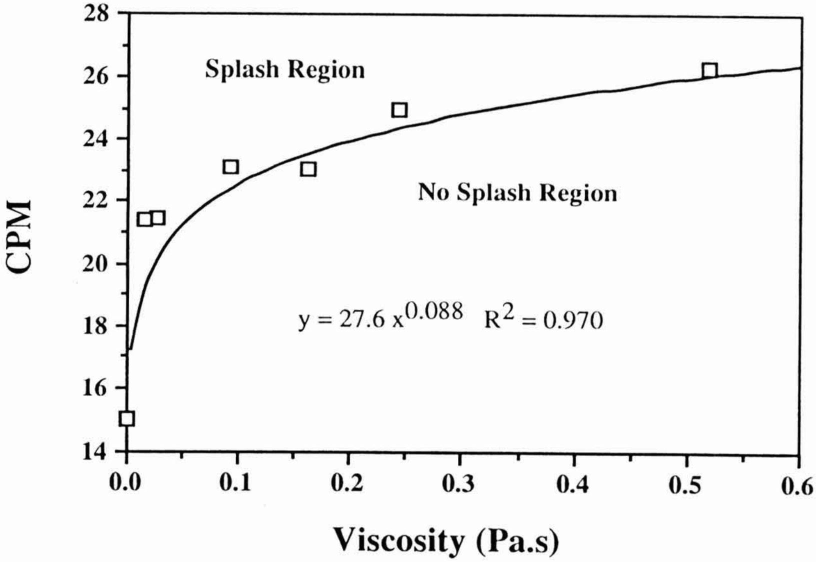

FIG. 7. VISCOSITY (Pa.s) OF NEWTONIAN FLUIDS VERSUS CYCLES/MIN (CPM) AT SPLASH FOR 295 ml OVAL CONTAINER

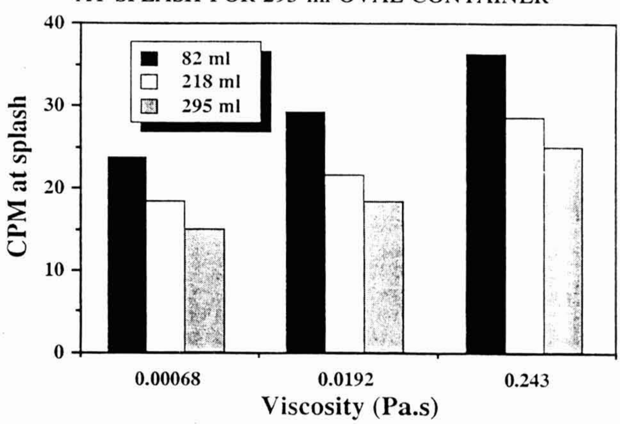

FIG. 8. BAR GRAPH SHOWING CYCLES/MINUTE (CPM) AT SPLASH FOR THREE NEWTONIAN FLUIDS AND THE THREE CONTAINERS

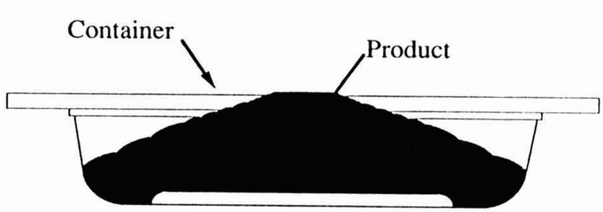

FIG. 9. ILLUSTRATION OF HEAPING FOODS WITH HIGH YIELD STRESS-PARTIAL SPREADING OF FOODS AND FLATTENING AT TOP BY PLUNGER ARE SHOWN

Figure 8 is a bar graph of the threshold CPM values, i.e., the CPM values at which splashing first occurred as a function of viscosity of Newtonian liquids for the three containers. It is readily seen in Fig. 8 that threshold CPM values were higher for lower fill volumes and higher food viscosities.

Splashing with Crushed Pineapple

Severe splashing occurred with crushed pineapple at two stages of the filling process: (1) first when the food hit the bottom of the container, and (2) again when the plunger hit the top of the heaped food. The primary cause for splashing was the large amount of liquid (juice) that separated from the crushed pineapple pieces. In general, the amount of splashed liquid in the case of crushed pineapple was more than that observed with other foods. Because phase separation is inherent to many foods, splashing will occur during filling of these foods. Efforts to minimize splashing should be based on minimizing phase separation.

Effect of High Insoluble Solids Foods on Filler Performance

Air Pockets in Foods. With the 29.7°Brix tomato paste, at both 32 and 39 C, it was found that pockets of air were introduced as the containers were filled with the food. The air pockets were formed in the storage tank when the rotor blade, which keeps the discharge port either open or closed, tunneled through the paste, instead of mixing the paste. The air pockets were formed due to the

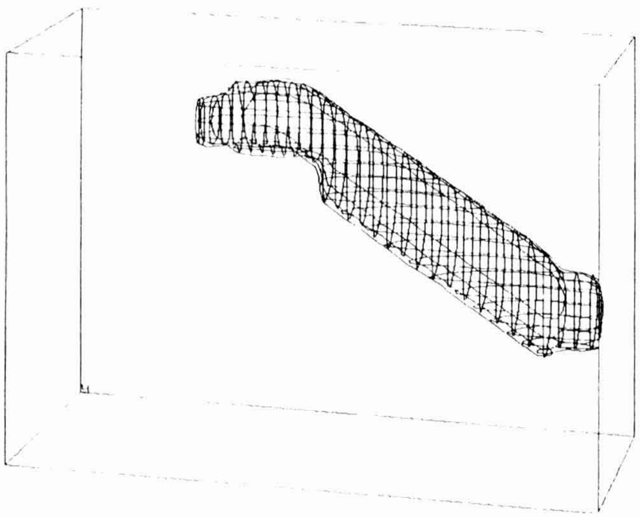

FIG. 10. COMPUTED FLUID SURFACE IN THE FILLER TUBE AT THE BEGINNING OF THE DISCHARGE STROKE

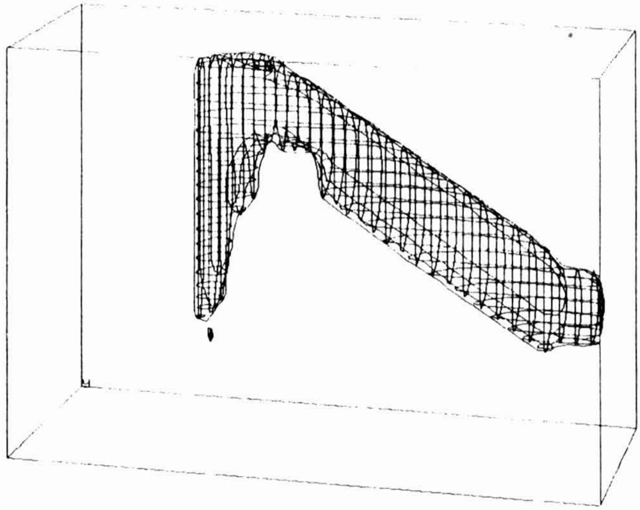

FIG. 11. COMPUTED FLUID SURFACE IN THE FILLER TUBE AND IN THE NOZZLE — NOTE THE DROPLET FORMED

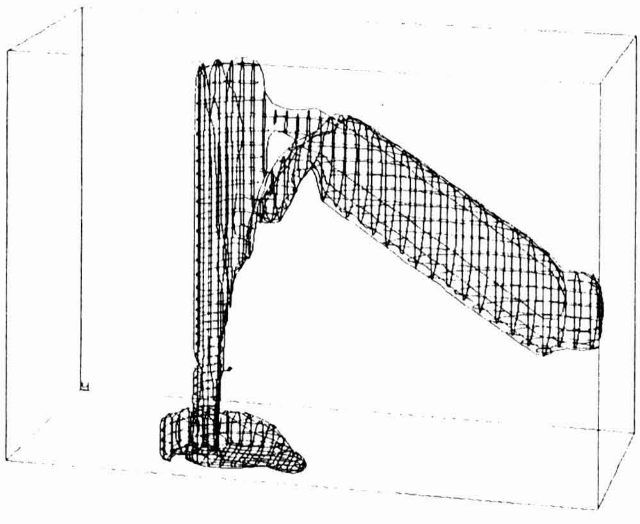

FIG. 12. COMPUTED FLUID SURFACE IN THE FILLER TUBE, THE NOZZLE, AND IN A CONTAINER

high shearing action that in turn was due to the high rate of rotation of the rotor blade. There was a physical separation of the paste with air spaces in several places in the storage tank. The air pockets within the paste were then sucked in by the piston and discharged into the container. With the 29.7 °Brix tomato paste, always a mixture of air and product was delivered, i.e., at no time did we observe only air being delivered to a container. Tunneling was also observed in another experiment with 30.3°Brix tomato paste at 154F (67.8C).

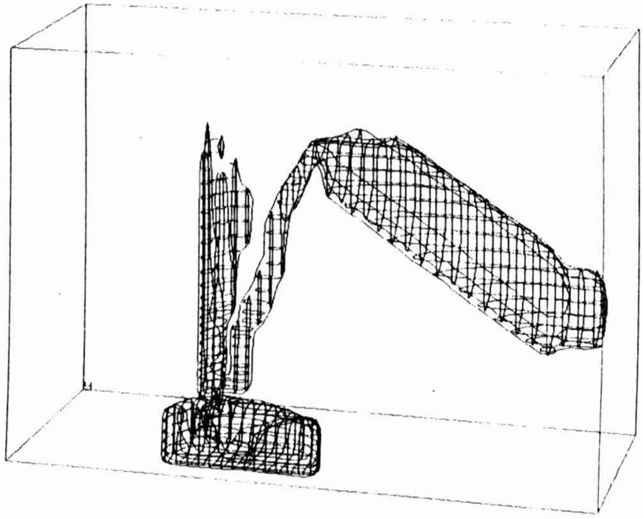

FIG. 13. COMPUTED FLUID SURFACE IN THE FILLER TUBE, THE NOZZLE, AND IN A CONTAINER--NOTE THAT THE FLUID HAS BEGUN TO BREAK UP

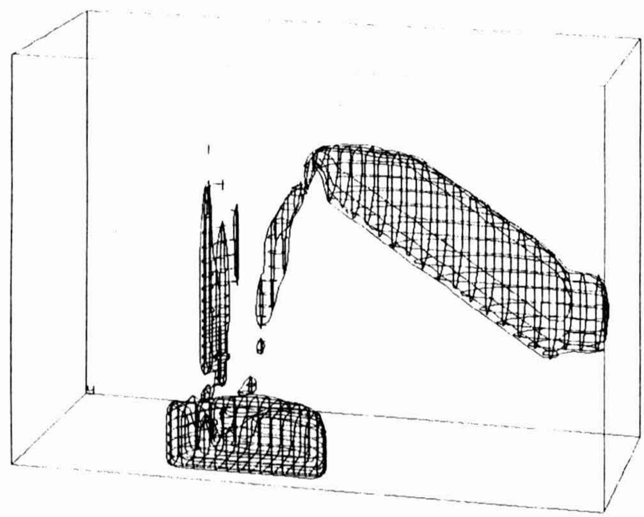

FIG. 14. COMPUTED FLUID SURFACE IN THE FILLER TUBE, THE NOZZLE, AND IN A CONTAINER—NOTE THAT THE FLUID SHOWS ADDITIONAL BREAKUP

In contrast to the observations with the 29.7°Brix tomato paste with a yield stress of about 180–205 Pa, no tunneling and pockets of air in the product delivered were found with a 23.8 °Brix tomato puree that had a yield stress of about 40 Pa. This suggests that when handling foods with high yield stresses (usually foods with high insoluble solids content), the current PN010 filler design contributes to air pockets being introduced during filling.

One recommendation from this study that is applicable for handling high-insoluble-solid foods is that the cross-section of the rotor blade and its rotation must be such that high-shear tunneling of the product is eliminated. It appears that tunneling, and consequent air pockets, can occur in products with insoluble solids content of about 30% and higher. We emphasize that this observation is valid for foods containing suspended solids and not for liquid foods with high solids content, such as concentrated apple juice.

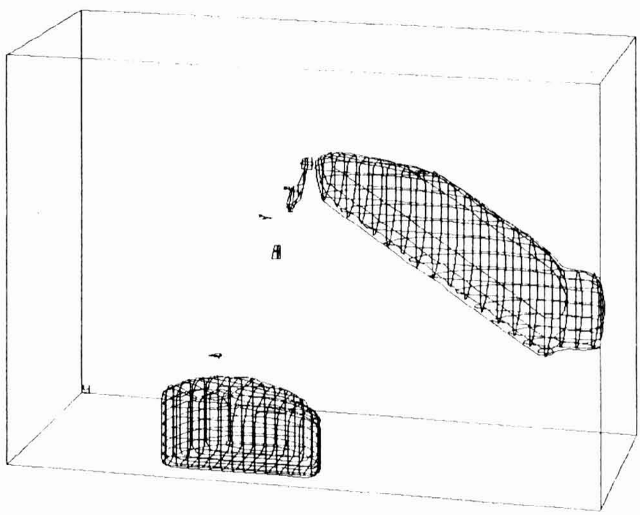

FIG. 15. COMPUTED FLUID SURFACE NEAR THE END OF FILLING CYCLE-NOTE THE FULL CONTAINER AND THE FEW DROPLETS EMERGING FROM THE NOZZLE

Heaping of Foods in Containers. With the 29.7°Brix tomato paste, the 23.8 and 16.3°Brix tomato purees, pork and beans, and dog food samples, the products were delivered into the container without splashing, but the products were heaped resulting in contact of the food with the plunger surface. The flat food surface created due to contact with the plunger surface is shown schematically in Fig. 9. Therefore, for these products the potential for dripping exists in a continuous operation. Heaping would also cause difficulty in closing the container.

Because the heaping phenomenon can be interpreted as the virtual absence of leveling and spreading, we suggest that heaping of a food in a container occurs when the food has a large value of yield stress. It is well known that with foods with high magnitudes of yield stresses, plug flow occurs during flow in a pipe, such as the nozzle of the PN010 filler (Rao and Anantheswaran 1982).

The food in the form of a plug is then delivered into the container where it does not level and spread easily. Our data suggests that heaping in the containers occurred for magnitudes of yield stresses of foods ≥ 29 Pa. In a continuous filling operation, such as in a processing plant, the dislodged food could fall on the rim of another container and cause potential problems. Sticking of foods to the plunger occurred to some extent with all foods, but it was more with dog food, and pork and beans.

Role of container in heaping. One interesting observation was that for all the foods studied, heaping was less severe with the small circular container with a height of 4 cm, in comparison with heights of 2.9 and 3.7 cm for the other two containers. This suggests that, when acceptable, deeper containers are desirable to minimize problems of heaping. This is because deeper containers can accommodate the plugs better than shallow containers. However, splashing was not affected very much by depth of containers.

Because heaping of foods in containers is dependent on a property of the foods, i.e., the yield stress, and it occurs after the food is discharged from the filler, changes in the filler design will not reduce or eliminate heaping. Therefore, attempts to counteract heaping must be done after the filling operation, such as applying vibration to the container or leveling the food in the container mechanically.

Computer Simulation Results

Detailed three-dimensional velocity profiles of the filling stream and free surface shapes during a filling cycle were computed (Figures 10-15). It should be noted that in Figures 10–15, only the fluid surfaces are shown, but the geometries of the filler walls and of the container are not shown. Figure 10 illustrates the fluid surface in the filler tube and in the nozzle at the beginning of a cycle. In Figure 11, the fluid surface has advanced into the nozzle; in addition, a drop can be seen. In Figure 12, the entry and spread of the food in a container, and the initial breakup of the food within the filler tube are shown. Further breakup of the food in the filler tube and the nozzle is illustrated in Figures 13 and 14. Figure 15 illustrates a full container and a few droplets emerging from the nozzle. In a continuous filling operation, the droplets formed during the breakup of a discharged food fall on the rim of the container being filled and/or that of the next container. Additional calculations from computer simulations, not shown here, verified the splash and no splash separation regions determined experimentally (Fig. 5–7). Further, as explained above, they provided insight into the mechanisms of splashing. The multiple jet phenomenon observed experimentally was also calculated.

CONCLUDING REMARKS

The viscosity and yield stress of foods affected splashing and heaping of foods in containers, respectively. Viscosity and filler speed at splash in CPM for three containers were related by power law relationships. Computer simulation provided a detailed view of flow during a filling cycle that could not be observed during experiments, such as that splashing was due to breakup of food into droplets in the filler tube and nozzle of the PN010 filler.

REFERENCES

HARLOW, F.H. and WELCH, J.E. 1965. Numerical calculation of time-dependent viscous incompressible flow. Phys. Fluids *8*, 2182-2189.

HIRT, C.W. and NICHOLS, B.D. 1981. Volume of fluid method for the dynamics of free boundaries. J. Computational Phys. *39*, 201-225.

HIRT, C.W. and SICILIAN, J. 1985. Flow-3D Users Manual, Flow Science Inc., Los Alamos, NM.

RAO, M.A. 1975. Measurement of flow properties of food suspensions with a mixer. J. Texture Studies *6*, 533-539.

RAO, M.A. and ANANTHESWARAN, R.C. 1982. Rheology of fluids in food processing. Food Technol. *36*(2), 116–126.

WELCH, J.E., HARLOW, F.H., SHANNON, J.P. and DALY, B.J. 1965. The MAC method. A computing technique for solving viscous, incompressible, transient fluid-flow problems involving free surfaces. Los Alamos Scientific Laboratory, Report LA-3425, Los Alamos. NM.

BULK VOLUME SHRINKAGE DURING DRYING OF WHEAT AND CANOLA

W. LANG and S. SOKHANSANJ[1]

Department of Agricultural and Bioresource Engineering
University of Saskatchewan
Saskatoon, SK S7N 0W0 Canada

Accepted for Publication May 21, 1993

ABSTRACT

The bulk volume shrinkage of canola and wheat were measured for the temperature range of 20–80C and relative humidity range of 15–90%. The volume decreased exponentially with time as seed moisture content was reduced. For canola, an oilseed, shrinkage and moisture reduction were linearly correlated with a shrinkage coefficient of about 1.0. For wheat, a starchy grain, the relationship was also linear but the coefficient was greater than 1.3. The shrinkage coefficients for both wheat and canola did not show a correlation with drying temperature but varied linearly with relative humidity of the drying air.

BACKGROUND

Several investigators have monitored the rate of shrinkage in bulk grain during moisture desorption. Miles (1937) dried shelled corn from 30% initial moisture content to 12% final moisture content and reported a volume shrinkage of 29%. Clark and Lamond (1968) related the one dimensional shrinkage of wheat to the mean moisture reduction and found:

$$\Delta X = 0.85\Delta M \qquad (1)$$

where ΔX was the relative bed shrinkage, and ΔM was the bed mean moisture reduction on a decimal dry basis.

Boyce (1965) proposed a shrinkage equation for barley dried from 34% to 14% in a 0.31 m^2 bed. A linear equation relating percentage shrinkage of the bed, ΔX, to the average moisture content, M, was developed:

[1]Contact author: Dr. S. Sokhansanj, Dept. of Agric. & Biore. Eng., University of Saskatchewan, Saskatoon, SK S7N 0W0 Canada, Phone: (306)966-5309, FAX: (306)966-5334.

$$\Delta X = 25.21 - 0.66M \quad (14\% < M < 34\%) \tag{2}$$

Bala and Woods (1984) presented an exponential model to describe the depth reduction in the bulk malting barley. The barley sample was dried at 50C and 12% relative humidity in a cylindrical column of 0.15 m diameter and 0.3 m deep. The shrinkage equation was presented in the following form:

$$\Delta X = 15.91(1 - e^{-0.97\Delta M}) \tag{3}$$

where ΔX was shrinkage and ΔM was moisture reduction, both in %.

No quantitative data are available in the literature on bulk volume shrinkage of canola. Furthermore, previous researchers did not study the effect of drying variables such as temperature and relative humidity of the air on the shrinkage of bulk wheat.

Mathematical drying models have been developed based on the assumption that the shrinkage in volume is negligible (Brooker *et al.* 1974). However, Spencer (1972) revised his earlier drying equations (Spencer 1969) to incorporate shrinkage (Eq. 1) and showed improvement in drying simulation.

In a preliminary test, we observed about 25% shrinkage when wheat and canola were dried from 20 to 10% moisture content in a 60 cm deep bed. A detailed investigation was undertaken to quantify the bulk volume shrinkage of wheat and canola during drying. The drying conditions encompassed a temperature range of 20–80C and a relative humidity range of 15–90%.

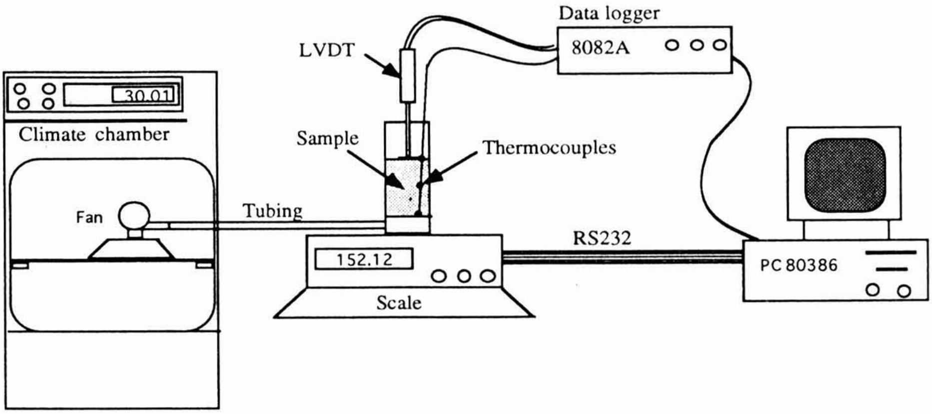

FIG. 1. SCHEMATIC DIAGRAM OF EXPERIMENTAL SETUP FOR MEASURING VOLUME SHRINKAGE AND MOISTURE CONTENT OF GRAIN DURING DRYING

MATERIALS AND METHODS

The laboratory equipment used for the drying and shrinkage measurements is illustrated schematically in Fig. 1. The system consisted of four components: a climate chamber, a cylindrical container, transducers, and the data acquisition. The function of the system was to expose a depth of grain mass in the sample container to an air stream and to continuously record changes in mass and depth of the sample.

The sample container was made of a 1 mm thick wall steel cylinder with 50 mm inside diameter and 150 mm height. The container and connecting tube were insulated to minimize heat loss. The container was mounted on an electronic scale to weigh the mass of sample within variation of ± 0.01 g.

The drying air was conditioned in a UY150 Climate Chamber (Angelantoni Climatic System, Italy) and was supplied to the test container by a small DC fan. The airflow rate was measured at the point of exit from sample container using a calibrated hot wire anemometer. Vertical displacement of the sample in the container was measured using a linear variable displacement transducer (LVDT). Three insulated 0.03 mm diameter T-type thermocouples were inserted into the grain to measure temperatures at the bottom, middle and top of the sample mass in the container.

Clean samples of Hard Red Spring wheat (*Triticum aestivum*) Kenyon variety and canola (*Brassica campestris*) Tobin variety were remoistened with water spray. The wet samples were conditioned for 48 h at room temperature in sealed containers. Moisture contents were determined by the air oven method to be 23.0% for wheat and 20.8% for canola after moistening. The fan speed was adjusted to deliver a constant airflow velocity of 0.1 m/s. Drying tests were conducted on each grain type using the air conditions listed in Table 1.

TABLE 1.
DRYING AIR CONDITIONS AND THE FINAL MOISTURE CONTENTS (%) OF WHEAT AND CANOLA

T (C)	RH (%)									
	15		30		50		70		90	
	wheat	canola	wheat	canola	wheat	canola	wheat	canola	wheat	canola
20	10.7	4.5	12.0	6.0	13.5	6.3	15.4	7.5	16.5	13.5
30	11.2	4.0	12.5	6.0	15.5	9.5	15.5	w	--	--
40	11.4	6.0	11.5	6.0	w	w	--	--	--	--
60	9.0	3.8	w	w	--	--	--	--	--	--
90	7.2	3.9	w	w	--	--	--	--	--	--

w: Grain did not dry.

--: Test was not conducted.

The listed temperatures and relative humidities were nominal values varying less than ±0.5C and ±2%, respectively. Initial mass of sample in the container was 131 ± 0.01 g for wheat and 120 ± 0.01 g for canola.

The measured vertical displacement and mass change of each sample were converted into volume shrinkage and moisture reduction. For each temperature, experiments were conducted at increasing relative humidity levels until wetting of the sample was observed. Table 1 shows that, at 20C, the wetting did not occur up to 90% relative humidity. But when temperature exceeded 40C, the wetting took place at 20% relative humidity.

RESULTS AND DISCUSSION

Volume Shrinkage

To study the temperature effect on bulk volume, dry grains with moisture content of 9.1% for wheat and 6.4% for canola were exposed to a air of 80C and 10% relative humidity. Figure 2 shows that the grain volumes changed randomly within the range of ±1.6% of their original values for both wheat and canola. The small variations in volume shown in Fig. 2 were suspected to be mainly due to random errors.

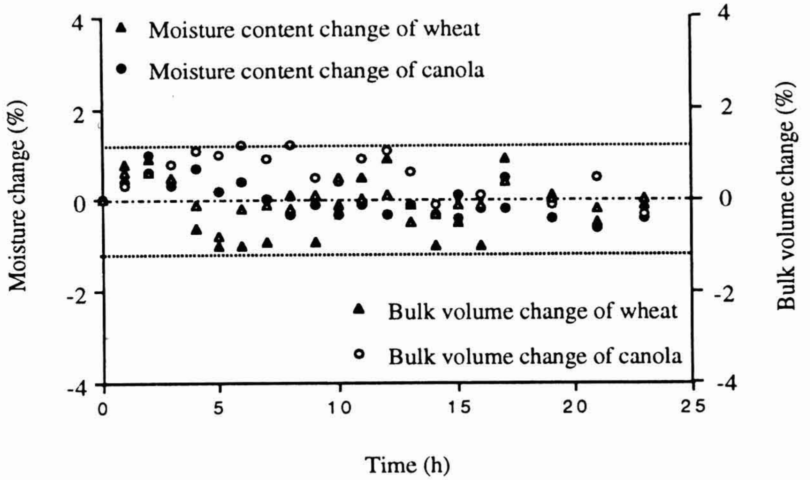

FIG. 2. THERMAL EXPANSION OF BULK VOLUME AND MOISTURE CHANGE OF WHEAT AND CANOLA AT 80C AND 10%RH
Initial moisture contents: 9.1% for wheat and 6.4% for canola.

When a moist grain was exposed to the drying air, the average shrinking rate, $\delta M/\delta t$, was related to the average drying rate, $\delta M/\delta t$:

$$\frac{\partial X}{\partial t} \propto \frac{\partial M}{\partial t} \tag{4}$$

The shrinkage coefficient was defined as the ratio of the volume shrinkage to the moisture reduction in a time step, Δt:

$$\lambda_m = \frac{\Delta X}{\Delta M} \tag{5}$$

where,

$$\Delta X = 100\,(X_i - X)/X_i,\ \% \tag{6}$$

$$\Delta M = M_i - M,\ \% \tag{7}$$

X_i and M_i were initial values of measured bed depth and measured average bed moisture content.

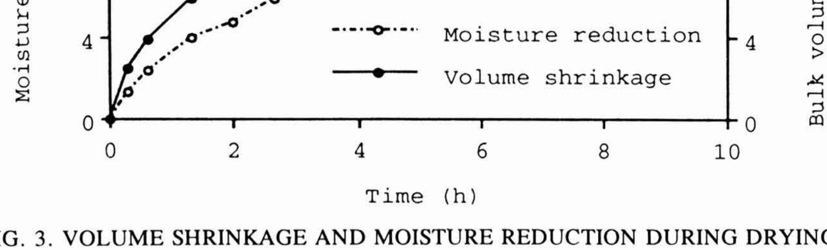

FIG. 3. VOLUME SHRINKAGE AND MOISTURE REDUCTION DURING DRYING OF WHEAT AT 30C and 30% RH

Shrinkage and Moisture Content

Figures 3 and 4 show the volume shrinkage and moisture reductions of wheat and canola during drying with air of 30C and 30% RH. The plotted data show that volume shrinkage and moisture reduction follow an exponential trend with time. For wheat, the shrinkage rate appeared to be faster than the moisture reduction rate. For canola, the shrinkage and moisture reduction were parallel.

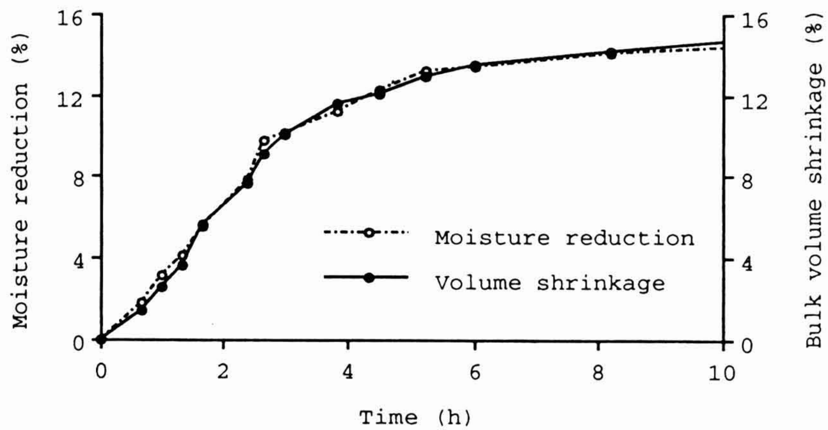

FIG. 4. VOLUME SHRINKAGE AND MOISTURE REDUCTION DURING DRYING OF CANOLA AT 30C AND 30%RH

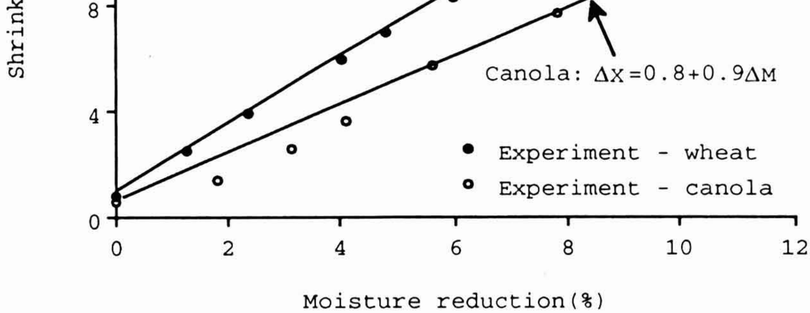

FIG. 5. RELATIONSHIP BETWEEN VOLUME SHRINKAGE AND MOISTURE REDUCTION OF WHEAT AND CANOLA DRIED AT 30C AND 30%RH

The linear relationship between the bulk shrinkage and the moisture reduction is evident from Fig. 5. The relationship can be expressed as:

$$\Delta X = \alpha + \lambda_m \Delta M \qquad (8)$$

where α may be considered as settlement constant.

The settlement may be caused primarily by airflow and vibration. The value of α was 1.0% for wheat and 0.8% for canola. Compared to the total shrinkage of 12–16%, the settlement effect on shrinkage calculation can be assumed negligible.

Dependence of shrinkage coefficient on air relative humidity and temperature is shown in Fig. 6(a) and (b). Estimated values of the shrinkage coefficients, λm, varied with relative humidity from 1.31 and 1.60 for wheat and from 0.96 to 1.37 for canola. The estimated shrinkage coefficients varied with temperature from 1.35 to 1.39 for wheat and from 1.01 to 1.07 for canola. The coefficients, λ_m, as functions of the air relative humidity and temperature, were statistically analyzed using a SAS (SAS 1990). The resulting correlation equations were found as follows:

for wheat:

$$\lambda_m = 1.3 + 0.4 \times 10^{-2} RH + 0.2 \times 10^{-3} T \quad (R^2 = 0.94) \qquad (9)$$

and for canola:

$$\lambda_m = 0.9 + 0.7 \times 10^{-2} RH + 0.3 \times 10^{-3} T \quad (R^2 = 0.90) \qquad (10)$$

where RH is the relative humidity, %, and T is air temperature, C.

The F-test showed that the dependence of the shrinkage coefficients on the air temperature was not statistically significant ($p = 0.05$).

Figure 6(a) also shows that the shrinkage coefficient of wheat was greater than that of canola. Physical structures and compositions of the two grains may have contributed to the differences in shrinkage. The hull of canola may limit the change in seed volume. Closing-down of the crease during drying of wheat may also be a major contribution to the greater volume change in wheat than in canola. Since canola contains 40% oil, the seed holds less water than wheat. The starch molecules in wheat provide strong polar sites to attract water molecules and expand.

Figure 7 shows that shrinkage as calculated using Eq. (1), (2), (3), (8), (9) and the data of the present work at 30% relative humidity. Compared to Clark and Lamond's (1968) Eq. (1) for wheat, the shrinkage coefficient calculated using Eq. (9) was about 38% larger. The shrinkage calculated from Eq. (2) for barley had the least slope and also showed a nonzero intercept. The nonzero intercept might be due to initial settlement of the bed. Equation (3) gave a rapid

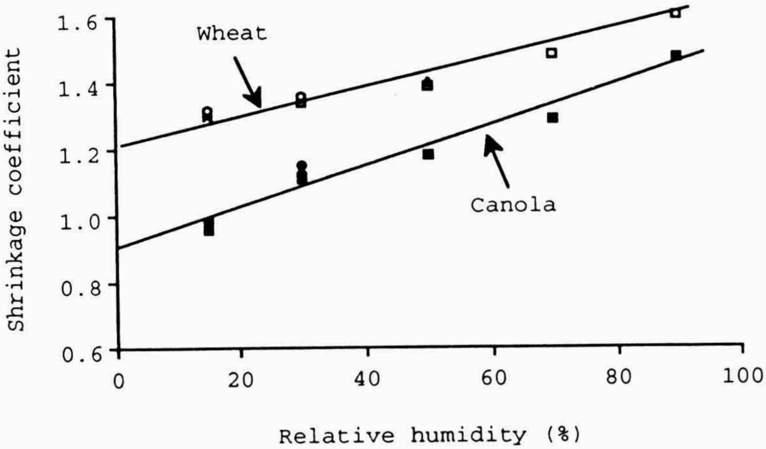

FIG. 6a. SHRINKAGE COEFFICIENT OF WHEAT AND CANOLA VERSUS AIR RELATIVE HUMIDITY

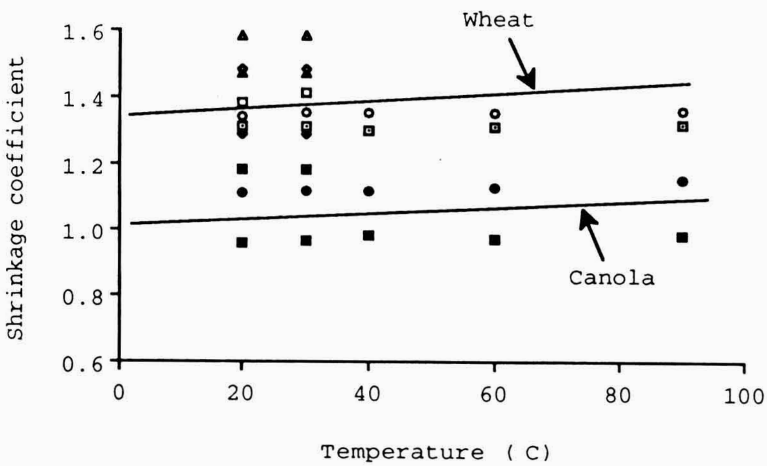

FIG. 6b. SHRINKAGE COEFFICIENT OF WHEAT AND CANOLA VERSUS AIR TEMPERATURE

shrinkage at the beginning of drying. When the moisture reduction approached 3%, the exponential term became small and shrinkage approached the steady state of 15.9%. It implied that, for malting barley, which is usually dried from 45 to 5%, the moisture reduction did not result in a proportional shrinkage throughout the drying process.

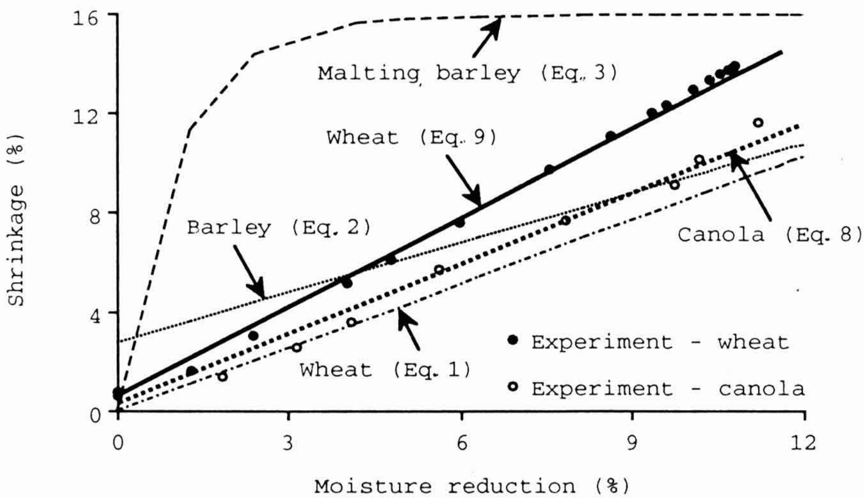

FIG. 7. COMPARISONS OF VOLUME SHRINKAGE FOR WHEAT, CANOLA AND BARLEY

CONCLUSIONS

From the present experiments on bulk volume shrinkage of wheat and canola during drying, the following conclusions can be drawn:

(1)The volume shrinkage and moisture reduction were linearly related in the form of $\Delta X = \alpha + \lambda \Delta M$.

(2)The statistical analysis based on the experimental data showed that the shrinkage coefficient was primarily a function of relative humidity for both wheat and canola.

(3) The magnitude of volume shrinkage of wheat was greater than that of canola during drying.

REFERENCES

BALA, B.K. and WOODS, J.L. 1984. Simulation of deep bed malt drying. J. Agric. Eng. Res. *30*, 235.

BALABAN, M. and PIGOTT, G. 1986. Shrinkage in fish muscle during drying. J. Food Sci. *51*, 510.

BOYCE, D.S. 1965. Grain moisture and temperature changes with position and time during through drying. J. Agric. Eng. Res. *10*, 333.

BROOKER, D.B., BAKKER-ARKEMA, F.W. and HALL, C.W. 1974. *Drying Cereal Grains*, Van Nostrand Reinhold/AVI, New York.

CLARK, R.G. and LAMOND, W.J. 1968. Drying wheat in 2 ft beds. J. Agric. Eng. Res. *13*(2), 141.

MILES, S.R. 1937. Test weight of corn. J. Am. Soc. Agron. *29*, 412.

SAS. 1990. SAS Users' Guide. Statistical Analysis System, Cary, NC.

SPENCER, H.B. 1969. A mathematical simulation of grain drying. J. Agric. Eng. Res. *14*(3), 226.

SPENCER, H.B. 1972. A revised model of the wheat drying process. J. Agric. Eng. Res. *17*, 189.

THERMAL INACTIVATION KINETICS OF TRYPSIN AT ASEPTIC PROCESSING TEMPERATURES

G.B. AWUAH, H.S. RAMASWAMY[1], B.K. SIMPSON and J.P. SMITH

Department of Food Science and Agricultural Chemistry
Macdonald Campus of McGill University
21,111 Lakeshore Rd., Ste Anne de Bellevue
Quebec, Canada, H9X 3V9

Accepted for Publication May 26, 1993

ABSTRACT

Kinetics of thermal inactivation of trypsin (bovine pancreas) were evaluated in the temperature range, 90–130C, common to aseptic processing of high/low acid foods. Aliquots of trypsin in buffer, at three pH values, 3.8, 5.1 and 6.0, were subjected to selected heat treatments at various temperatures. Kinetic parameters were evaluated from the residual enzyme activity. Reference k and D values (at 121.1C) ranged from 0.0719 to 0.349 min^{-1} and 32.0 to 6.6 min, and E_a and z values ranged from 84.9 to 69.9 kJ/mole and 33.1 to 39.9C, respectively, in the pH range 3.8–6.0. The thermal inactivation resistance of trypsin in the acid and low acid pH range makes it a potential bioindicator for high temperature thermal processes.

INTRODUCTION

Thermal processing is an important technique for shelf-life extension of both low and high acid foods. The primary purpose is to produce a commercially sterile product by destroying pathogenic microorganisms while creating an environment to suppress the growth of others. Quality improvements in thermally processed products have been made possible through adaptation of HTST/UHT, thin profile, rotational as well as aseptic processing principles. Since temperature measurement of moving particles is a serious problem, aseptic processing of particulate foods rely on microbiological/biological validations (Dignen *et al.* 1989). Problems associated with the use of microorganisms as bioindicators have been detailed in several studies (Weng *et al.* 1991a,b; Pflug and Odlaug 1978; Berry *et al.* 1989; Sastry *et al.* 1988).

[1]Contact Person: H. Ramaswamy, Associate Professor; Tel. 514-398-7919; Fax 514-398-7977

Journal of Food Process Engineering **16** (1993) 315–328.

Process optimization has been traditionally attempted through studies on the destruction of nutrients/enzymes. Mulley *et al.* (1975) used thiamine hydrochloride as a chemical index to evaluate sterilization efficacy. Textural changes in meat was used as a heating index by Tennigen and Olstad (1979). Berry *et al.* (1989) studied the destruction kinetics of methyl methionine sulfonium (MMS) in buffer solutions and found it to be suitable for indexing microbial lethality. They recommended MMS as a substitute for microorganisms in thermal process evaluation.

The activation energy associated with microorganisms is higher than for nutrients and enzymes. Therefore, the rate of destruction of microorganisms proceeds more rapidly as temperature increases in comparison to destruction of enzymes and nutrients (Schwartz 1992). For high-temperature short-time processing, it might be necessary to use enzymes as indicators rather than microbial spores and nutrients. For vegetable processing, peroxidase inactivation is often used as indicator due to its reported heat stability.

Trypsins are a family of enzymes that catalyze preferentially the hydrolysis of ester and peptide bonds involving the carboxyl groups of L-lysine and L-arginine with serine and a histidine residue participating in the mechanism of catalysis (Keil 1971; Richardson and Hyslop 1985). Trypsin has been isolated from several sources of food including cow, sheep, turkey, fish and pigs (Simpson and Haard 1984; Northrop *et al.* 1948; Travis 1968).

Thermal inactivation studies related to trypsin have often been carried out with respect to its inhibitors, which are usually inactivated at pasteurization temperatures (van der Poel *et al.* 1990; Rao *et al.* 1989; Soetrisno *et al.* 1982). According to Keil (1971), trypsin is most stable at pH 3.0. Northrop (1932) indicated that solutions of crystalline trypsin exhibit a remarkable property quite different from other enzymes: in dilute acid solutions (pH 1.0 - 7.0), trypsin can be heated to boiling with little or no loss in activity, and without apparent formation of any denatured protein. Simpson and Haard (1984) found that bovine trypsin retained virtually all its activity after 30 min heating at 80C. Activation energy ranged from 46.5–56.1 kJ/mole depending on the substrate and concentration of calcium ions used. A search of the literature indicates that there is lack of data on effect of heat on trypsin at different pH in the thermal processing temperature range (90–130C).

The objectives of this work were to study (1) the thermal inactivation kinetics of trypsin in the pH range covering both low and high acid foods, and (2) to evaluate the possibility of using trypsin as a bioindicator for aseptic processes.

MATERIALS AND METHODS

Enzyme and Chemicals

Bovine pancreas trypsin (type III) and benzoyl-DL-arginine p-nitroanilide (BAPA) were obtained from Sigma Chemical Co. (St. Louis, MO). Tris (hydroxy-methyl-amino-methane) was obtained from ICN Biochemicals (Cleveland, MO). Calcium chloride and dimethyl sulfonide (DMS) were obtained from Anachemia Science (Montreal, Canada).

Enzyme Assay

The amidase activity of trypsin was assayed using the method of Erlanger *et al.* (1961). BAPA served as the substrate. The reaction mixture consisted of 0.2 ml of enzyme solution and 2.8 ml of BAPA substrate (dissolved in DMS) in 0.05 M Tris-HCI buffer (pH 8.2) containing 0.02 M $CaCl_2.2H_2O$. The increase in light absorption was measured with a Beckman D*υ* 7500 diorray spectrophotometer at 410 nm and 25C. Control experiments were run using 0.2 ml 1 mM HCI or citrate buffer, instead of enzyme, and 2.8 ml of the substrate.

Heat Treatment

Trypsin dissolved in dilute 1 mM HCl (pH 3.8) or citrate buffer (pH 5.1, and 6.0) was appropriately adjusted to give similar activity on the substrate. Aliquots of trypsin were sealed in 2 ml glass ampoules (Canlab Canada, Montreal, PQ) using a gas flame and immediately submerged in ice/water mixture. Initial studies showed that the sealing process had no effect on the initial enzyme activity. Heating was done in a well-agitated constant temperature oil bath. Temperatures studied were 90, 100, 110, 120, and 130C. For a given temperature, samples were taken from the oil bath at 5 min intervals for pH 3.8 and 5.1 and 1 min intervals at pH 6.0 and cooled immediately in an ice/water mixture. Prior to enzyme assay for residual activity, the sample temperature was equilibrated to 25C.

Needle type copper-constantan thermocouples (Ecklund-Harrison Technologies, Cape Coral, FL) were inserted into the ampoules and sealed with silicone glue. Time-temperature data were gathered during the come-up period and heating times were corrected for the lag period prior to kinetic data analyses.

Kinetic Data Analysis

Thermal inactivation of trypsin was assumed to follow a first order kinetic process expressed as:

$$\log_e[A/Ao] = -kt \tag{1}$$

where A = enzyme activity (change in optical density/min), t = time (min), Ao = initial enzyme activity and k = reaction rate constant (min^{-1}). k values were obtained as negative slopes of $\log_e[A/Ao]$ vs. t regression.

The decimal reduction time (D-value, time needed to reduce 90% of the activity) was calculated from:

$$D = 2.303/k \tag{2}$$

The half-life ($t_{1/2}$) was calculated from the expression:

$$t_{1/2} = 0.693/k \tag{3}$$

The temperature dependence of rate constants were analyzed by both Arrhenius and thermal death time (TDT) concepts. For the Arrhenius model, the activation energy E_a(kJ/mole) was obtained from the slope of the semi-logarithmic plot of Eq. (4):

$$k = s\, e^{-E_a/RT} \tag{4}$$

where s = frequency factor, k = reaction rate constant (min^{-1}), T = absolute temperature (K), and R = universal gas constant (8.314 x 10^{-3} kJ/mole K). From the D value curve, z-value (temperature range required to change D by 90%) was calculated from the relationship:

$$\log [D_1/D_2] = (T_2-T_1)/z \tag{5}$$

where T_2 and T_1 are temperatures corresponding to D_2 and D_1.

Heating times (t_{actual}) were corrected based on the duration (t_{CUT}) and effectiveness fraction (E) of come-up period using procedure adopted by Nath and Ranganna (1977):

$$t_{corrected} = t_{actual} - t_{CUT} * (1-E) \tag{6}$$

Briefly, the following procedure was adopted: For a given pH with its associated uncorrected D and z-values, enzyme inactivation contributed during the come-up period was evaluated from the gathered time-temperature data. Come-up effectiveness was calculated as the fraction of accumulated inactivation during come-up period divided by the theoretical inactivation that would have been contributed by instantaneous exposure at bath temperature for the same period. Heating times were corrected using Eq. (6), and D-values and z values were recalculated. Based on corrected D and z-values, the effectiveness was again recalculated and the entire procedure was repeated until the difference between the previous and recent D and z values were less than 0.5%.

Trypsin versus Microbial and Other Enzyme Kinetics

Two approaches were used to compare the destruction kinetics of trypsin with other indicators, as well as to demonstrate its utility in aseptic processing applications. First, the decimal reduction time equivalencies (1D) of various indicators and *Bacillus stearothermophilus* were compared at various temperatures with respect to equivalent heating time (EHT) at 121.1C using a z = 10C (which is the same as process lethality or F_o value as commonly employed in thermal processing). In order to do this, first the decimal reduction times of enzyme activity or microbial population were calculated at various temperatures based on their respective D_o and z values:

$$D_T = D_0 * 10^{[(121.1 - T)/z]} \quad (7)$$

The corresponding equivalent heating times (EHT) at the reference temperature of 121.1C were then calculated assuming the traditional reference z value of 10C:

$$EHT = D_T * 10^{[(T - 121.1)/10]} \quad (8)$$

The second approach was to compare residual activities of various bioindicators following a standard heat process. An F_o value (process lethality) of 10 min (commonly employed in several thermal processing applications) was chosen for this purpose. The percentage residual activity (RA) of the bio-indicator was evaluated using a reverse approach to Eq. 7 & 8. The heating time (F_T, z = 10C) at various temperatures equivalent to an F_o of 10 min were first calculated:

$$F_T = 10 * 10^{[(121.1 - T)/10]} \quad (9)$$

This was then coupled with the corresponding decimal reduction time (D_{Tq}) obtained from Eq. (7) to compute the percentage residual activity:

$$RA(\%) = 10^{(2.0 - F_T/D_T)} \quad (10)$$

Data on kinetic parameters for the different indicators were obtained from literature. D_0 and z values were, respectively, for peroxidase — 12.94 min and 31.39C (Adams 1978); MMS at pH 6.0 — 7.53 min and 20.0C (Berry *et al.* 1989); *Bacillus stearothermophilus* at pH 5.0 — 4.0 min and z = 7.8C, and at pH 6.0 — 5 min and 12.2C (Stumbo 1973; Berry *et al.* 1989).

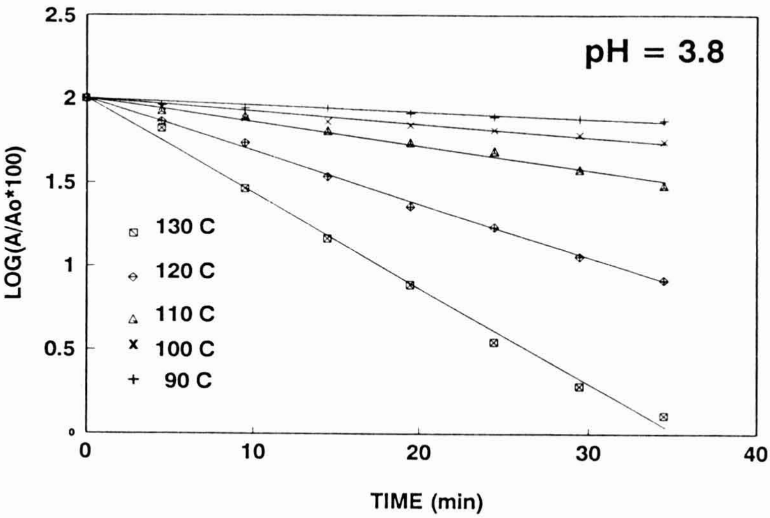

FIG. 1. RESIDUAL ACTIVITY AS A FUNCTION OF HEATING TIME AT VARIOUS TEMPERATURES FOR TRYPSIN IN DILUTE HCl (pH = 3.8)

RESULTS AND DISCUSSION

Figures 1–3 show the first order plots of percent residual activity of trypsin at various pH as a function of time at five inactivation temperatures. With the exception of data at 90C for pH 5.1, the associated R^2 were higher than 80% (Table 1). Lenz and Lund (1980) reported that when the half-life (time needed to destroy 50% of initial activity) of an enzyme is $\leq$ 20 min, significant inactivation of enzyme occurs during the lag or come-up period. The half-life of trypsin was generally lower than 20 min under most experimental situations in this study (Table 1). Therefore, correction to the come-up (lag) period was necessary. The come-up times were approximately 95 s and come-up period effectiveness varied from 0.65 to 0.68. Generally, D-values decreased with increasing pH and temperature. For example, as the pH increased from 3.8 to 6.0, the D-value decreased by 5.5 times at 130C.

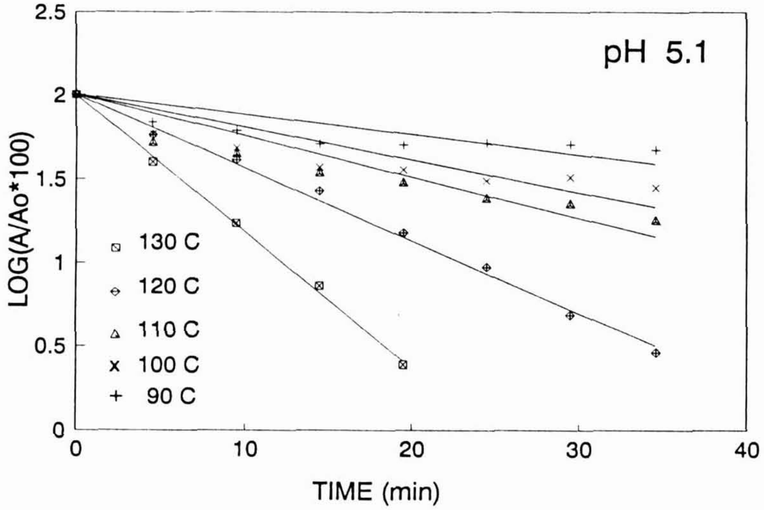

FIG. 2. RESIDUAL ACTIVITY AS A FUNCTION OF HEATING TIME AT VARIOUS TEMPERATURES FOR TRYPSIN IN CITRATE BUFFER SOLUTION (pH = 5.1)

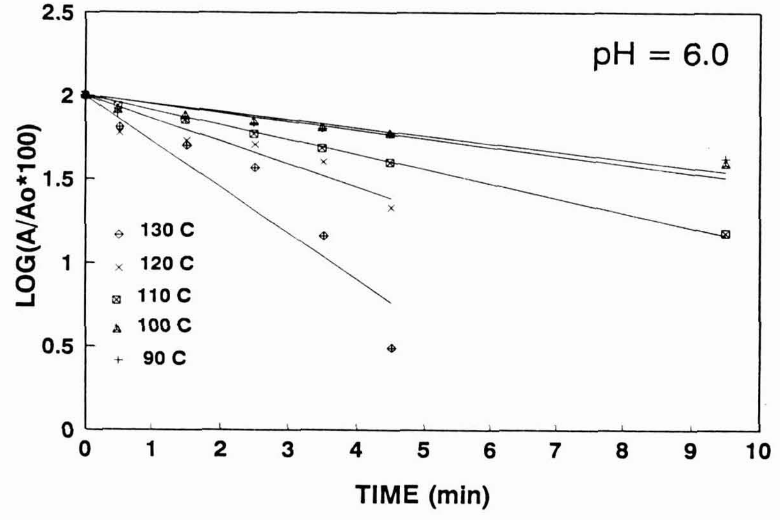

FIG. 3. RESIDUAL ACTIVITY AS A FUNCTION OF HEATING TIME AT VARIOUS TEMPERATURES FOR TRYPSIN IN CITRATE BUFFER SOLUTION (pH = 6.0)

Figure 4 shows TDT curves for the pH range studied. The Arrhenius plots (not shown) gave somewhat similar fit. The R^2 values obtained for z and E_a values (Table 2) indicate that Arrhenius and TDT models were somewhat comparable in spite of their contradictory nature with respect to describing the temperature dependence of kinetic parameters (in Arrhenius model, the kinetic parameter on logarithmic scale is inversely proportional to temperature, while in TDT approach the proportionality is direct). This observation supports that made by Ramaswamy *et al.* (1989) with regard to the models providing similar results. Simpson and Haard (1984) reported lower E_a values for trypsin than found in this study, possibly due to the low temperature range (5–35C) and high pH (8.2–9.5) conditions employed in their study.

TABLE 1.
KINETIC PARAMETERS FOR TRYPSIN IN DILUTE HCl AND CITRATE BUFFER

pH	temperature (C)	D-value (min)	k-value (min^{-1})	$t_{1/2}$ (min)	R^2
3.8	90	279.7	0.008233	84.17	0.96
	100	144.0	0.015998	43.32	0.97
	110	68.9	0.033413	20.74	0.99
	120	31.5	0.073153	9.47	0.99
	130	18.4	0.125396	5.53	0.99
5.1	90	132.0	0.017449	39.72	0.71
	100	72.8	0.031643	21.90	0.83
	110	50.8	0.045099	15.37	0.96
	120	22.8	0.101223	6.85	0.99
	130	11.7	0.196330	3.53	0.99
6.0	90	33.3	0.069271	10.00	0.79
	100	27.9	0.082585	8.39	0.90
	110	11.8	0.194773	3.56	0.99
	120	8.5	0.270479	2.56	0.87
	130	3.4	0.687139	1.01	0.90

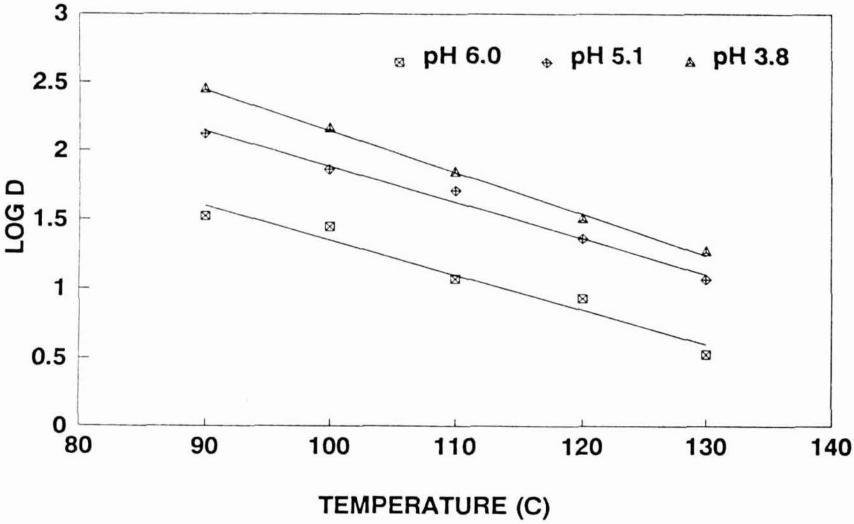

FIG. 4. THERMAL INACTIVATION TIME CURVES FOR TRYPSIN IN RELATION TO pH

The z-values were pH dependent and increased by approximately 20% between pH 3.8 and 5.1. Thereafter, there was only a marginal increase up to 6.0 (Table 2). The marginal differences can be observed from the seemingly similar slopes (Fig. 4). The activation energy dropped with pH in consistence with its reciprocal relationship with z value (Table 2). Again, the difference between activation energy at pH 5.1 and 6.0 was marginal.

Due to lack of published data on trypsin inactivation in the literature, comparative verification of the present results was difficult. The utility of the kinetic data were, however, evaluated on the basis of its similarity to other chemical, biochemical and microbiological validators (MMS, peroxidase and *Bacillus stearothermophilus*).

Lu and Whitaker (1974) found that thermal inactivation of horseradish peroxidase was pH dependent. At pH 3.5, all activity was lost within 0.5 min at 76C, and the rate of inactivation decreased eight times when the pH was increased from 4.0 to 7.0. For peroxidase inactivation of low-acid fruits and vegetables (Schwimmer 1981), z values ranged from 8.8 to 71.9C. For acid foods, values ranged from 10F (~5.6C) to 34F (~18.9C). Adams (1978) reported z, E_a, and D_0 values for horseradish peroxidase (RZ = 3.2) to be 31.4C, 29.6 kcal/mole, and 12.94 min, respectively (in acetate buffer at pH 5.6 and temperatures ranging from 70 to 150C). The z-values for trypsin fell in the range reported for peroxidase in low-acid fruits and vegetables. The D_0 value reported by Adams (1978) falls in the range found for trypsin in citrate buffer at pH 5.1 and 6.0 (Table 2).

TABLE 2.
ACTIVATION ENERGY (E_a), z VALUES, D_0, K_0 AND THEIR CORRESPONDING R^2 VALUES FOR TRYPSIN IN DILUTE HCl OR CITRATE BUFFER SOLUTIONS

pH	Temperature (C)	E_a (kJ/mole)	k_o (min^{-1})	R^2	z C	D_o (min)	R^2
3.8	90 - 130	84.9	0.071969	0.99	33.1	32.0	0.99
5.1	90 - 130	72.8	0.106620	0.98	38.4	21.6	0.99
6.0	90 - 130	69.9	0.348939	0.95	39.9	6.6	0.96

Figure 5 shows variations in EHT values representing one decimal reduction in the activity of trypsin, *Bacillus stearothermophilus*, peroxidase and MMS, plotted as a function of temperature. The decimal reduction EHTs at 130C of the various indicators in the increasing order of resistance were as follows: 2.24 min (*Bacillus stearothermophilus*); 21 min (MMS); 30.7 min (trypsin at pH 6), 52.3 min (peroxidase); 98.3 min (trypsin at pH 5.1) and 135 min (trypsin at pH 3.8). EHT values represent the equivalent heating times at the reference temperature of 121.1C, which should be differentiated from the decimal reduction times at the condition in question. In the above example the real D values were: 0.29, 2.7, 3.95, 6.7, 12.7 and 17.2 min. EHT concept has been used in this analysis to get a more realistic comparison of the inactivation behavior of various enzymes at different temperatures because the process times are based on F_0 calculated using a z value of 10C while the enzyme inactivation is characterized by its own characteristic D_0 and z values. As is evident from Fig. 5, the order of resistance to thermal destruction of different bioindicators are not the same at different temperatures. At lower temperatures, *Bacillus stearothermophilus* has a higher thermal resistance than all other indicators with an EHT value of 11.4 min as compared to 0.4–2.4 min for the others, while the trend reverses as processing temperatures exceed 120C. At the high temperatures employed for aseptic processing, therefore, enzymes serve as better indicators for the verification of the process.

In Fig. 6, the extent of inactivation/destruction of various indicators in a process with equivalent F_0 of 10 min are compared. The residual activity/concentration of all the enzymes as well as MMS were higher than *Bacillus stearothermophilus*. At the aseptic processing temperature of 130C,

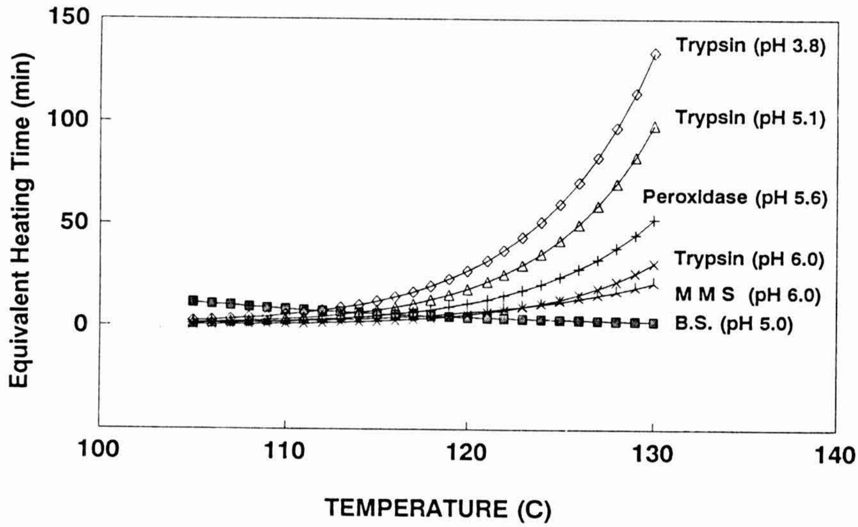

FIG. 5. EQUIVALENT HEATING TIME (EHT) FOR A DECIMAL REDUCTION IN ACTIVITY OF TRYPSIN AND SELECTED BIOINDICATORS AT VARIOUS TEMPERATURES

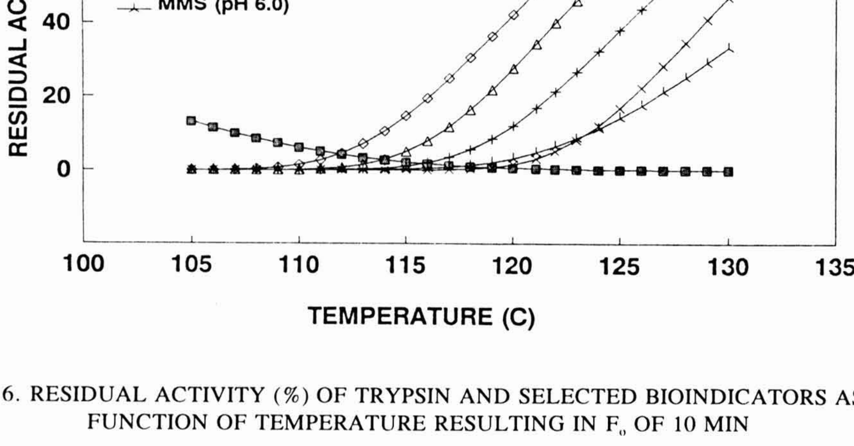

FIG. 6. RESIDUAL ACTIVITY (%) OF TRYPSIN AND SELECTED BIOINDICATORS AS A FUNCTION OF TEMPERATURE RESULTING IN F_0 OF 10 MIN

approximately 47% of the original trypsin activity was retained at pH 6.0 while at pH 3.8 the residual trypsin activity was as high as 84%. Percentage retention of MMS and peroxidase at 130C were 33 and 64% respectively with the corresponding pH values of 6.0 and 5.6. Accurate measurement of residual activities of all these enzymes in the range mentioned above is possible. These results indicate that trypsin, especially at pH 6, with its associated thermal resistance characteristics approximately between those of MMS and peroxidase, can be a good candidate for biovalidation purposes.

Although microbiological verification and validation are the final criteria in aseptic processes, it may be prudent to consider enzymes as indicators because of their convenience in handling and evaluation.

CONCLUSIONS

Thermal inactivation of trypsin has been shown to follow a first order reaction over the pH range studied. Data obtained could be described by both the TDT and Arrhenius models. Results indicate that trypsin is heat resistant with pH dependent thermal kinetics. The thermal resistance of trypsin, especially at pH 6, is somewhat comparable to that of peroxidase and MMS. This makes trypsin a potential bioindicator for low acid foods.

ACKNOWLEDGMENTS

This research was supported by grant from the Strategic Grant Program of Natural Science and Engineering Research Council of Canada. Canadian International Development Agency provided financial assistance to the first author.

REFERENCES

ADAMS, J. B. 1978. The inactivation and regeneration of peroxidase in relation to the high temperature short-time processing of vegetables. J. Food Technol. *13*, 281.

BERRY, M. F., SINGH, R. K. and NELSON, P. E. 1989. Kinetics of methylmethionine sulfonium in buffer solutions for estimating thermal treatment of liquid foods. J. Food Processing Preservation *13*, 475.

DIGNEN, D.M., BERRY, M. R., PFLUG, I.J. and GARDINE, T.D. 1989. Safety considerations in establishing aseptic processes for low-acid foods containing particulates. Food Technol. *43*(3), 118–121, 131.

ERLANGER, B, F., KOKOWSKY, N. AND COHEN, W. 1961. The preparation and properties of two new chromogenic substrates of trypsin. Arch. Biochem. Biophys. *95*, 271–278.

KIEL, B. 1971. Trypsin. In *The Enzymes,* Vol. iii, (P.D. Boyer, ed.) p. 249-275, Academic Press, New York.

LENZ, M. K. and LUND, D. B. 1980. Experimental procedure for determining destruction kinetics of food components. Food Technol. *34*(2), 51.

LU, A. T and WHITAKER, J. R. 1974. Some factors affecting rates of heat inactivation and reactivation of horseradish peroxidase. J. Food Sci. *39*, 1173–1178.

MULLEY, E. A., STUMBO, C. R. and HUNTING, W. M. 1975. Kinetics of thiamine degradation by heat. J. Food Sci. *40*, 985.

NATH, S. and RANGANNA, S. 1977. Evaluation of thermal process for acidified canned muskmelon (*Cucumis melo* L.) J. Food Sci. *42*, 1306.

NORTHROP, J. H. 1932. Crystalline trypsin. IV. Reversibility of the inactivation and denaturation of trypsin by heat. J. Gen. Physiol. *16*, 323.

NORTHROP, J. H., KUNITZ, M. and HERRIOT, R. 1948. *Crystalline Enzymes*, 2nd Ed., pp. 125–167, Columbia University Press, New York. pp.125-167.

PFLUG, I. J. and ODLAUG, T. E. 1978. A review of z and F values used to ensure safety of low-acid canned food. Food Technol. *32*(6), 63.

RAMASWAMY, H. S., VAN DE VOORT, F. R. and GHAZALA, S. 1989. Analysis of TDT and Arrhenius methods for handling process and kinetic data. J. Food Sci. *54*, 1322.

RAO, V., DESTEFANO, M. V., PEREZ, C. R. and BARREIRO, J. A. 1989. Kinetics of thermal inactivation of protease (trypsin and Chymotrypsin) inhibitors in Black Beans (*Phaseolus vulgaris*) flour. J. Food Eng. *9*(13), 535.

RICHARDSON, T. and HYSLOP, D.B. 1985. Enzymes. In *Food Chemistry*, 2nd Ed. (O.R. Fennema, ed.) p. 455. Marcel Dekker, Inc. New York.

SASTRY, S.K., *et al.* 1988. A bio-indicator for verification of thermal processes for particulate foods. J. Food Sci. *53*(5), 1528.

SCHWARTZ, S. J. 1992. Quality consideration during aseptic processing of foods. In *Advances in Aseptic Processing Technologies*, (R.K. Singh and P.E. Nelson, eds.) p. 63, Elsevier Applied Science, New York.

SCHWIMMER, S. 1981. *Source Book of Food Enzymology*, p. 206, Van Nostrand Reinhold/AVI, New York.

SIMPSON, B. K. and HAARD, H. F. 1984. Trypsin from Greenland Cod, *Gadus ogac*. Isolation and comparative properties. Comp. Biochem. Physiol. 79B, 613–622.

SOETRISNO, U., HOLMES, Z. A. and MILLER, L. T. 1982. Effect of heating time of soybean on vitamin B6 and folacin retention, trypsin inhibitor activity, and microstructure changes. J. Food Sci. *47*, 530.

STUMBO, C. R. 1973. *Thermobacteriology in Food Processing*, 2nd Ed., Academic Press, New York.

TENNIGEN, A. and OLSTAD, S. 1979. Computer controlled heating of meat with respect to protein denaturation. In *Food Process Engineering*, Vol. 1. Food Processing Systems, (C.P Linko *et al.* eds.) Applied Science Publ., London.

TRAVIS, J. 1968. Studies on the active site of sheep trypsin. Biochem. Biophys. Res. Commun. *30*, 730–734.

VAN DER POEL, T.F.B., VAN ZUITCHEM, D.J. and VAN OORT, M.G. 1990. Thermal inactivation of lecithins and trypsin inhibitor activity during steam processing of dry bean (*Phaseolus vulgaris*) and effects on protein quality. J. Food Agric. *53*, 215.

WENG, W.M., HENDRICKX, M., MAESMANS, G. and TOBBACK, P. 1991a. Immobilized peroxidase: a potential bio-indicator for evaluation of thermal processes. J. Food Sci. *56*(2), 567.

WENG, W. M., HENDRICKX, M., MAESMANS, G. and TOBBACK, P. 1991b. Thermostability of soluble and immobilized horseradish peroxidase. J. Food Sci. *56*(2), 574.

AUTHOR INDEX

Journal of Food Process Engineering **16** (1993) 329–330.

SUBJECT INDEX

Journal of Food Process Engineering **16** (1993) 331-332.

FNP

PUBLICATIONS IN FOOD SCIENCE AND NUTRITION

Journals

JOURNAL OF FOOD LIPIDS, F. Shahidi
JOURNAL OF RAPID METHODS AND AUTOMATION IN MICROBIOLOGY, D.Y.C. Fung and M.C. Goldschmidt
JOURNAL OF MUSCLE FOODS, N.G. Marriott and G.J. Flick, Jr.
JOURNAL OF SENSORY STUDIES, M.C. Gacula, Jr.
JOURNAL OF FOODSERVICE SYSTEMS, C.A. Sawyer
JOURNAL OF FOOD BIOCHEMISTRY, J.R. Whitaker, N.F. Haard and H. Swaisgood
JOURNAL OF FOOD PROCESS ENGINEERING, D.R. Heldman and R.P. Singh
JOURNAL OF FOOD PROCESSING AND PRESERVATION, D.B. Lund
JOURNAL OF FOOD QUALITY, J.J. Powers
JOURNAL OF FOOD SAFETY, T.J. Montville and A.J. Miller
JOURNAL OF TEXTURE STUDIES, M.C. Bourne and P. Sherman

Books

S.C. PRESCOTT, M.I.T. DEAN AND PIONEER FOOD TECHNOLOGIST, S.A. Goldblith
FOOD CONCEPTS AND PRODUCTS: JUST-IN-TIME DEVELOPMENT, H.R. Moskowitz
MICROWAVE FOODS: NEW PRODUCT DEVELOPMENT, R.V. Decareau
DESIGN AND ANALYSIS OF SENSORY OPTIMIZATION, M.C. Gacula, Jr.
NUTRIENT ADDITIONS TO FOOD, J.C. Bauernfeind and P.A. Lachance
NITRITE-CURED MEAT, R.G. Cassens
POTENTIAL FOR NUTRITIONAL MODULATION OF AGING, D.K. Ingram *et al.*
CONTROLLED/MODIFIED ATMOSPHERE/VACUUM PACKAGING OF FOODS, A.L. Brody
NUTRITIONAL STATUS ASSESSMENT OF THE INDIVIDUAL, G.E. Livingston
QUALITY ASSURANCE OF FOODS, J.E. Stauffer
THE SCIENCE OF MEAT AND MEAT PRODUCTS, 3RD ED., J.F. Price and B.S. Schweigert
HANDBOOK OF FOOD COLORANT PATENTS, F.J. Francis
ROLE OF CHEMISTRY IN THE QUALITY OF PROCESSED FOODS, O.R. Fennema, W.H. Chang and C.Y. Lii
NEW DIRECTIONS FOR PRODUCT TESTING OF FOODS, H.R. Moskowitz
PRODUCT TESTING AND SENSORY EVALUATION OF FOODS, H.R. Moskowitz
ENVIRONMENTAL ASPECTS OF CANCER: ROLE OF MACRO AND MICRO COMPONENTS OF FOODS, E.L. Wynder *et al.*
FOOD PRODUCT DEVELOPMENT IN IMPLEMENTING DIETARY GUIDELINES, G.E. Livingston, R.J. Moshy, and C.M. Chang
SHELF-LIFE DATING OF FOODS, T.P. Labuza
ANTINUTRIENTS AND NATURAL TOXICANTS IN FOOD, R.L. Ory
UTILIZATION OF PROTEIN RESOURCES, D.W. Stanley *et al.*
VITAMIN B_6: METABOLISM AND ROLE IN GROWTH, G.P. Tryfiates
POSTHARVEST BIOLOGY AND BIOTECHNOLOGY, H.O. Hultin and M. Milner

Newsletters

MICROWAVES AND FOOD, R.V. Decareau
FOOD INDUSTRY REPORT, G.C. Melson
FOOD, NUTRITION AND HEALTH, P.A. Lachance and M.C. Fisher
FOOD PACKAGING AND LABELING, S. Sacharow

CONTENTS